

University of Texas at Arlington

MavMatrix

Civil Engineering Dissertations

Civil Engineering Department

2023

Proactive Seismic Rehabilitation Decision-Making Model for Water Pipe Networks Under Network Uncertainties and Degradation

Abhijit Roy

Follow this and additional works at: https://mavmatrix.uta.edu/civilengineering_dissertations



Part of the [Civil Engineering Commons](#)

Recommended Citation

Roy, Abhijit, "Proactive Seismic Rehabilitation Decision-Making Model for Water Pipe Networks Under Network Uncertainties and Degradation" (2023). *Civil Engineering Dissertations*. 496.
https://mavmatrix.uta.edu/civilengineering_dissertations/496

This Dissertation is brought to you for free and open access by the Civil Engineering Department at MavMatrix. It has been accepted for inclusion in Civil Engineering Dissertations by an authorized administrator of MavMatrix. For more information, please contact leah.mccurdy@uta.edu, erica.rousseau@uta.edu, vanessa.garrett@uta.edu.

**Proactive Seismic Rehabilitation Decision-Making Model for Water Pipe Networks Under
Network Uncertainties and Degradation**

by

Abhijit Roy

Dissertation

Submitted in partial fulfillment of the requirements

for the degree of Doctor of Philosophy at

The University of Texas at Arlington

December 2023

Arlington, Texas

Supervising Committee:

Dr. Mohsen Shahandashti, Supervising Professor

Dr. Mohammad Najafi

Dr. Nilo Tsung

Dr. Jay Rosenberger

Acknowledgments

I would like to thank my academic advisor and mentor, Dr. Mohsen Shahandashti, for his continued support, guidance, and supervision. My completion of PhD would not have been accomplished without his vision, encouragement, and faith in me. He has been an immensely good mentor to me, and I have been fortunate to obtain ample opportunities to improve my understanding of scientific research and life in general. I have been privileged to have him as my supervisor and will always be indebted for the guidance and support he provided me during my PhD program.

I would also like to thank my committee members Dr. Mohammad Najafi, Dr. Nilo Tsung, and Dr. Jay Rosenberger for being part of my PhD program and providing their insightful comments, advice, and contribution to my dissertation.

My sincere thanks also go to my friends and colleagues at UTA. I was blessed with lab mates who are real friends and a constant source of inspiration. I am always thankful for the precious experience at UTA.

I would like to cherish the memory of my father-in-law, who had tremendous confidence in me and always supported me during the short period of time I had the chance to talk with him.

My appreciation also goes to my family, especially my parents, mother-in-law, and my brother for their unwavering support, prayers, faith, and belief in me.

I also want to thank my wife, Shatabdi Saha, for her unconditional love and for dealing with my frequent absence over the past few years. Without her dedication and love, it would not have been possible for me to accomplish this research work.

Lastly, I am grateful to the National Science Foundation (NSF) for funding my studies at UTA. This project is partially supported by the National Science Foundation under Grant CMMI-1926792 and National Science Foundation I-corps project 1261007660.

Abstract

Proactive Seismic Rehabilitation Decision-Making Model for Water Pipe Networks Under Network Uncertainties and Degradation

Abhijit Roy

The University of Texas at Arlington, 2023

Supervising Professor: Mohsen Shahandashti

Past earthquakes have revealed that earthquakes disrupt operations of underground water infrastructure systems. Assessment of the seismic vulnerability of underground water pipe networks plays a critical role in formulating preventive rehabilitation decision making to ensure maximum serviceability after an earthquake event and avoid high repair costs. Although existing seismic vulnerability assessment methods and seismic rehabilitation decision-making models are sensitive to water pipe network uncertainties (e.g., uncertainties in nodal demand, reservoir head, and pipe roughness coefficient) and pipes' degradation, the extent of the effects of the network uncertainties and pipes' degradation on the postearthquake serviceability of the network and seismic rehabilitation decision-making has not been examined. The serviceability and damage of a water network after a seismic event depends on the hydraulic properties and physical properties of the network. The hydraulic properties and physical properties of the network are sensitive to network uncertainties and degradation. So, it is necessary to investigate the effects of network uncertainties and degradation of proactive seismic rehabilitation decision-making of water distribution networks. This research is divided into three sections to investigate the effects of water networks uncertainties and pipes' degradation on seismic vulnerability assessment models and seismic rehabilitation decision-making. In the first section, this research investigates the effects of water pipe network uncertainties on the seismic vulnerability assessment of networks. The approach was tested on two networks (New York Tunnel Network and Oberlin Network). The statistical analysis results indicated that the combined impact of the three selected water pipe network uncertainties on the seismic vulnerability assessment of networks is statistically significant. Nodal demand and pipe roughness coefficient uncertainties did not individually have a statistically significant effect. The individual effect of reservoir head uncertainty was statistically significant. Sensitivity analysis determined the minimum value of the coefficient of variation to

have a statistically significant effect. The results from sensitivity analysis showed that a small uncertainty in reservoir head results in a statistically significant effect on seismic vulnerability assessment. By contrast, the coefficient of variation for uncertainties in nodal demand and pipe roughness has to be quite large to significantly affect seismic vulnerability assessment. The next section aims to explore the impacts of water network uncertainties on proactive seismic rehabilitation decision-making. Pipe roughness coefficient, demand, and reservoir head were selected as uncertain network parameters for this study. Critical pipes were identified for a limited budget constraint considering these three network uncertainties individually and combinedly. Sensitivity analysis was performed to quantify selected network uncertainties. A stochastic combinatorial optimization problem was formulated considering network uncertainties and seismic ground motion intensities to identify the most critical pipes of a network for limited rehabilitation budget. A simulated-annealing algorithm was used to solve the stochastic combinatorial optimization problem. Modena network was used to demonstrate the method. The optimization results showed that the selected network uncertainties significantly affect the identified critical pipes of the water pipelines. Also, the maximum achievable serviceability index for selected rehabilitation budget reduces significantly if network uncertainties are considered. This index has been reduced by 3%–4% due to the consideration of all three network uncertainties. This third part of the research aims to investigate the effects of the degradation of pipes on the seismic rehabilitation decision-making of water distribution networks. Simulation experiments were designed to investigate the effects of degradation on the inside surface of pipes and on the outside surface of pipes individually and combinedly. Seismic repair rate was calculated considering the effects degradation based on the probabilistic stress change of pipe with age. The probabilistic nature of the pipes' outside degradation rate was considered to determine the probabilistic value of stress change. A probabilistic pipe roughness growth rate model was used to modify the hydraulic modeling of pipe considering pipes' inside degradation. A simulated annealing-based optimization approach was used to identify the critical pipes and associated maximum serviceability for each experiment and each budget constraint. The Analysis of Variance (ANOVA) test and Tukey statistical tests were conducted to identify the statistical significance of the effect of integrating degradation. The application of the proposed approach was illustrated on Modena network. Five rehabilitation budget constraints were selected for this study. Critical pipes were identified for each rehabilitation budget constraint based on the optimization algorithm. The

results for each simulation experiment showed that the identified critical pipes were different. The associated maximum serviceability was reduced for the same budget constraints if outside and inside degradation was considered individually and combinedly. The changes in identified critical pipes and associated maximum serviceability due to the consideration of outside and inside degradation implies the dependency of proactive seismic rehabilitation decision-making model on outside and inside degradation. The statistical test results imply that the degradation of pipes of the water distribution network has an impact on seismic rehabilitation decision-making models of water distribution networks. Therefore, it is recommended to integrate the degradation effect with existing seismic rehabilitation decision-making models.

Table of Contents

Acknowledgments.....	i
Abstract.....	ii
List of Figures.....	viii
List of Tables.....	x
CHAPTER 1 : INTRODUCTION.....	1
CHAPTER 2 : BACKGROUND.....	5
2.1. Existing seismic vulnerability assessment models.....	5
2.2. Effect of network uncertainties on design phase and operational phase.....	6
2.3. Existing water pipe degradation model.....	7
2.4. Gaps in knowledge.....	8
2.5. Research Objective.....	9
CHAPTER 3 : EFFECT OF NETWORK UNCERTAINTY ON SEISMIC VULNERABILITY ASSESSMENT OF WATER PIPE NETWORKS.....	10
3.1. Methodology.....	10
3.1.1. Uncertainty Identification and Quantification.....	11
3.1.2. Design of Experiments.....	12
3.1.3. Seismic Repair Rate Calculation.....	13
3.1.4. Integrated Multi-physics Modeling and Monte Carlo Simulation.....	16
3.1.5. Statistical Analysis of the SSI Database.....	19
3.2. Application and Results.....	19
3.3. Sensitivity Analysis.....	26
3.3.1. Effect of Individual Water Pipe Network Uncertainties.....	26
3.3.2. Joint Effect of Water Pipe Network Uncertainties.....	27
3.3.3. Combined Effect of Three Water Pipe Network Uncertainties.....	29
3.4. DISCUSSION.....	29

CHAPTER 4 : IMPACT OF WATER NETWORK UNCERTAINTIES ON SEISMIC REHABILITATION DECISION-MAKING FOR WATER PIPELINES	31
4.1. Methodology	31
4.1.1. Selection of Network	32
4.1.2. Uncertainty Quantification	32
4.1.3. Design of Experiments	33
4.1.4. Calculating PSSI for Each Random PGV Field	33
4.1.5. Determining a Sufficient Number of Monte Carlo Runs	35
4.1.6. Optimization Problem Formulation.....	35
4.2. Results and discussion.....	37
4.3. DISCUSSION	41
CHAPTER 5 : EFFECTS OF DEGRADATION ON SEISMIC REHABILITATION DECISION-MAKING FOR WATER PIPE NETWORKS.....	42
5.1. METHODOLOGY.....	43
5.1.1. Design of Simulation Experiment	43
5.1.2. INTEGRATION OF EFFECT OF DEGRADATION ON OUTSIDE SURFACE OF PIPE.....	44
5.1.3. Integration of Effect of Degradation on Inside Surface of Pipes	46
5.1.4. Seismic Rehabilitation Decision-Making.....	48
5.1.5. Statistical Analysis to Investigate the Effect of Degradation	50
5.2. APPLICATION AND RESULTS.....	51
5.2.1. Selection of Network.....	51
5.2.2. Assumptions for this study	52
5.2.3. Cost Boundaries.....	53
5.2.4. Deaggregation Analysis and Calculation of PGV	53
5.2.5. Selection of the maximum number of Monte Carlo runs:	54

5.2.6. Results: Identification of Critical Pipes.....	55
5.2.7. Results: Statistical Analysis.....	60
5.3. DISCUSSION	61
CHAPTER 6 : CONCLUSION	63
6.1. Summary of Results	63
6.2. APPLICATION TO INDUSTRY	65
6.3. Future Work	66
REFERENCES	67

List of Figures

Figure 1.1: General methodology of existing proactive seismic rehabilitation decision-making model.....	2
Figure 3.1: Methodology for investigating effects of network uncertainties.....	11
Figure 3.2: Steps of calculating seismic repair rate of each pipe.....	14
Figure 3.3: Steps of Monte Carlo simulation to create SSI database for each experiment for a given earthquake scenario for the mth PGV field.....	18
Figure 3.4: Layout of New York Tunnel network	20
Figure 3.5: Layout of Oberlin network	20
Figure 3.6: Peak ground velocity field due to the selected earthquake scenario without intraevent and interevent residuals.....	21
Figure 3.7: Peak ground velocity field due to the selected earthquake scenario without intraevent and interevent residuals zoomed to network scale for New York Tunnel network.....	21
Figure 3.8: Peak ground velocity field due to the selected earthquake scenario without intraevent and interevent residuals zoomed to network scale for Oberlin network.....	22
Figure 3.9: Convergence study using Oberlin network to identify sufficient Monte Carlo runs .	23
Figure 3.10: Result of sensitivity analysis with two water pipe network uncertainties (a) demand and pipe roughness coefficient for New York Tunnel network (b) demand and pipe roughness coefficient for Oberlin network (c) pipe roughness coefficient and reservoir head	28
Figure 3.11: Result of sensitivity analysis with three water pipe network uncertainties (a) New York Tunnel network (b) Oberlin network.....	29
Figure 4.1: Methodology of exploring the impacts of water network uncertainties on optimal seismic rehabilitation decision-making.....	31
Figure 4.2: Layout of Modena network	32
Figure 4.3: Peak ground velocity field due to the selected earthquake scenario without intraevent and interevent residuals.....	34
Figure 4.4: Peak ground velocity field due to the selected earthquake scenario without intraevent and interevent residuals zoomed to network scale for Modena network.....	34
Figure 4.5: Result of convergence study.....	35
Figure 4.6: Critical pipes identified for different experiments (Budget \$2.5 million)	38

Figure 4.7: Critical pipes identified for different experiments (Budget \$5 million)	39
Figure 4.8: Critical pipes identified for different experiments (Budget \$7.5 million)	40
Figure 4.9: Critical pipes identified for different experiments (Budget \$10 million)	41
Figure 5.1: Steps of calculating the probabilistic value of Hazen-Williams roughness coefficient for pipe p after year T (CpT).....	48
Figure 5.2: Steps of determining the value of $E[PSSI(x)]$ for each rehabilitation policy and average PSSI for each PGV field	50
Figure 5.3: Layout of Modena network	52
Figure 5.4: Layout of Modena network with ages (in year) of different pipes.....	53
Figure 5.5: Summary of convergence study result	54
Figure 5.6: Value of maximum $E[PSSI]$ for each cost boundary	55
Figure 5.7: Identified critical pipes for different experiments using a cost boundary of 2.5 million	56
Figure 5.8: Identified critical pipes for different experiments using a cost boundary of 5 million	56
Figure 5.9: Identified critical pipes for different experiments using a cost boundary of 7.5 million	57
Figure 5.10: Identified critical pipes for different experiments using a cost boundary of 10 million	58
Figure 5.11: Identified critical pipes for different experiments using a cost boundary of 12.5 million.....	59

List of Tables

Table 3.1: Water network uncertainty models in the literature	11
Table 3.2: Water pipe network uncertainties with their levels for the experiment.....	13
Table 3.3: Design matrix of the experiment	13
Table 3.4: Mean and variance of SSI of each experiment for New York Tunnel network	23
Table 3.5: Mean and variance of SSI of each experiment for Oberlin network	24
Table 3.6: Results of Tukey test for New York Tunnel network.....	25
Table 3.7: Results of Tukey HSD test for Oberlin network	25
Table 3.8: Minimum value of CoV for each network uncertainties	26
Table 4.1: Sensitivity analysis result	33
Table 4.2: Name of the experiments along with design matrix	33
Table 4.3: Rehabilitation costs adopted for this study	36
Table 4.4: Maximum expected PSSI and actual cost of rehabilitation (Budget \$2.5 million)	37
Table 4.5: Maximum expected SSI and actual cost of rehabilitation (Budget \$5 million)	38
Table 4.6: Maximum expected SSI and actual cost of rehabilitation (Budget \$7.5 million)	39
Table 4.7: Maximum expected SSI and actual cost of rehabilitation (Budget \$10 million)	40
Table 5.1: Types of degradation in pipes with their levels of experiment.....	43
Table 5.2:Simulation experiment design matrix.....	44
Table 5.3: Typical statistical information of physical properties in pipeline analysis.....	46
Table 5.4: Properties of Modena network.....	51
Table 5.5: Summary of solution of simulated annealing optimization.....	59
Table 5.6: Summary of Tukey test result.....	60

CHAPTER 1 : INTRODUCTION

Water pipe networks are among the lifelines of modern cities (Eidinger and Avila 1999). Past earthquakes (e.g., the San Fernando earthquake of 1971, the Northridge earthquake of 1994, the Kobe earthquake of 1995) and some recent earthquakes (e.g., the Christchurch earthquake of 2011, the East Japan earthquake of 2011, the Gorkha earthquake of 2015, and the Central Mexico earthquake of 2017) have divulged the vulnerability of the underground water pipe networks (Knight 2017; Thapa et al. 2016; O' Rourke et al. 2014; Maruyama et al. 2011; Cubrinovski et al. 2011; O'Rourke 1996). Residential, industrial, and commercial activities get disrupted due to the damage to the water pipe networks. Earthquake impacts on water supply networks can result in enormous direct losses (e.g., cost of repair) and indirect losses (e.g., disruption in water distribution) (Yerri et al. 2017) and severely limit capacity to control conflagrations following earthquakes (Selina et al. 2008). In the Northridge earthquake of 1994, utilities performed around 1400 repairs in water pipes, of which approximately 100 repairs were carried out in pipes with large diameters (O'Rourke 1996). About 50,000 people were disconnected from the drinkable water supply for over seven days after the Northridge earthquake (Scawthorn et al. 2005). The Kobe earthquake caused damage at 23 locations of the water pipeline (Yoo et al. 2016). These facts highlight the significance of seismic vulnerability assessment of water pipe networks and mitigation of such vulnerabilities. A seismic vulnerability assessment of water supply networks estimates the likelihood of damage to pipelines and degradation of service after seismic events. Several seismic vulnerability assessment models have been proposed to address these challenges. Figure 1.1 shows a general methodology of existing proactive seismic rehabilitation decision-making model.

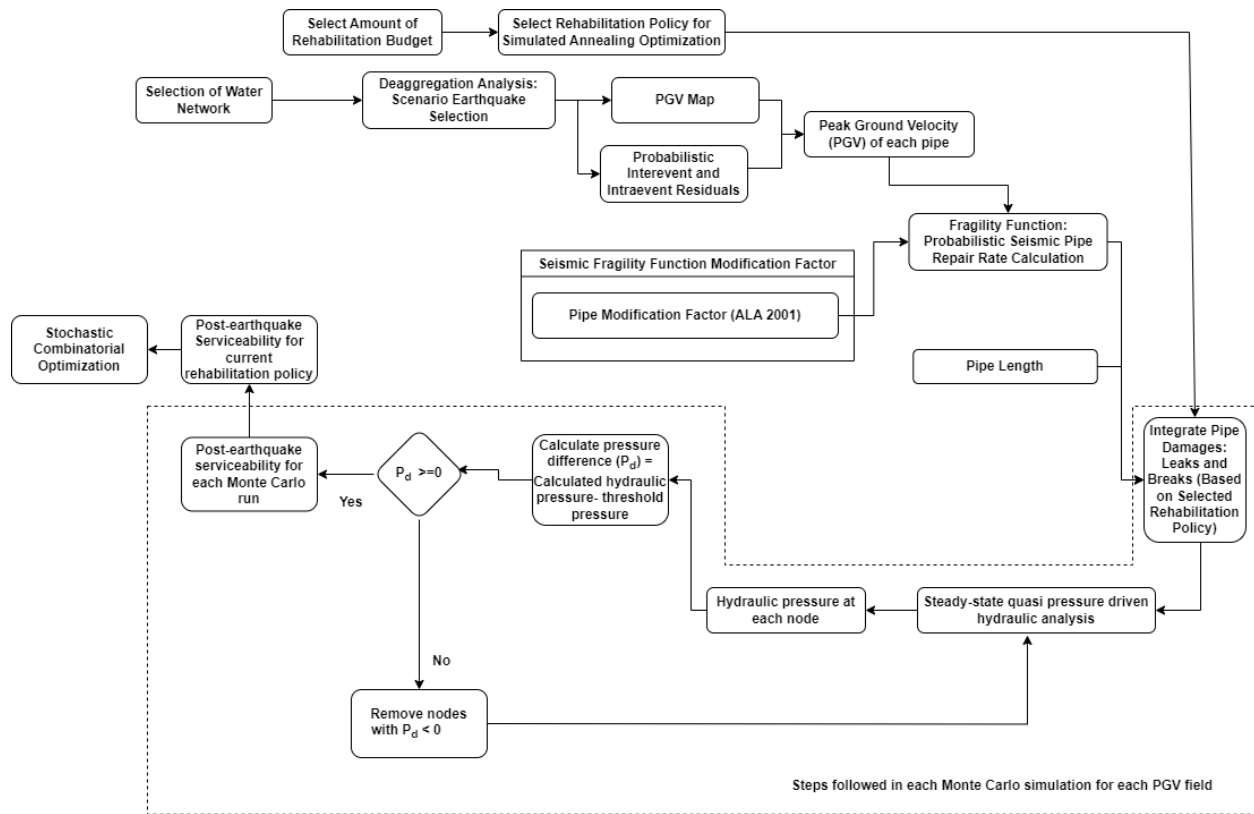


Figure 1.1: General methodology of existing proactive seismic rehabilitation decision-making model

In the current practice of vulnerability assessment of underground water pipe networks subjected to seismic events, it is implicitly assumed that currently established hydraulic network analysis models can accurately estimate reliability and serviceability measures. However, several studies have identified significant shortcomings of the hydraulic models representing actual networks (Sabzkouhi and Haghghi 2016; Seifollahi-Aghmiuni et al. 2013; Lansey et al. 2001; Bargiela and Hainsworth 1989). These shortcomings are mostly due to the high sensitivity of hydraulic models to their input variables. The bottleneck is the highly limited knowledge about the actual input values, which drive the hydraulic models. These values include nodal demands, pipe roughness coefficients, reservoir head, pipe material, pipe age, and pipe diameter (Kang and Lansey 2009, Shibu and Janga Reddy 2011). Sabzkouhi and Haghghi (2016) showed that a slight 15% uncertainty in a demand and pipe's roughness coefficient could cause around 11% deviation in predicted nodal pressures and 50% deviation in flow velocities. These results represent the high sensitivity of network hydraulic analysis models to uncertainties. Therefore, it is crucial to investigate the effects of water pipe network uncertainties on seismic vulnerability assessment of the networks.

Current seismic rehabilitation decision-making models depend a lot on the network hydraulics and seismic fragility curves to integrate the damages with the original network and to determine the pipe failure rate, respectively. Hydraulic modeling of water distribution networks depends on the pipe internal roughness (Christensen 2009; Abdel-Monim et al. 2005), while the seismic fragility curve depends on time-dependent maximum tensile stress on pipes (Ji et al. 2017). Although internal roughness of pipes and maximum tensile stress on pipes can be affected by degradation, existing seismic rehabilitation decision-making models ignored the effects of degradation.

United States' drinking water distribution network comprises of 2.2 million miles (about 3,540,556.8 km) of underground pipes to supply reliable water to people. The average age of the 1.6 million miles (about 2574950.4 km) of pipes in the United States is 45 years (ASCE Infrastructure Report Card 2021).

Due to this aging effect, degradation along the outside surface of the pipes and deposition along the internal surface of the pipes can change the maximum stress on the pipe (Ji et al. 2017) and the roughness of the pipe (Christensen 2009). Therefore, it is essential to investigate the effects of pipes' degradation on seismic rehabilitation decision-making of water distribution networks. Due to the random nature of the degradation and deposition, the probabilistic effects of degradation should be integrated with seismic rehabilitation decision-making.

The ultimate goals of this research are to (i) characterize and integrate the water pipe network uncertainties with a seismic vulnerability assessment model and identify the effects on the maximum serviceability of a water pipe network; (ii) identify the effects of network uncertainties on seismic rehabilitation decision-making of water pipe networks.; (iii) identify the effects of water pipe on seismic rehabilitation decision-making of water pipe networks. The works performed to achieve the goals of the research are outlined in the following ways.

Chapter 2 provides a comprehensive review of the literature on existing seismic vulnerability assessment and seismic rehabilitation decision-making models, effects of water pipe network uncertainties on design phase and operational phase, and existing water pipe network degradation models. Chapter 2 also provides the gaps in knowledge and research objective. Chapter 3 discusses the methodology of identification and quantification of water pipe network uncertainties and integrating them with an existing seismic vulnerability assessment model. Chapter 3 also presents the application of the model by applying it to existing water networks and identifying the effects

of water pipe network uncertainties integration by conducting statistical tests. Chapter 4 proposes a methodology to identify the roles of water pipe network uncertainties in identifying critical pipes of water pipe networks for proactive seismic rehabilitation decision-making. Chapter 4 also presents the application of the model by applying it to an existing water network and identifying the critical pipes of water pipe networks for proactive seismic rehabilitation decision-making. Chapter 5 proposes a methodology to identify the roles of water pipe network degradation on the maximum serviceability of a water pipe network for a predefined resource-constraint and on identifying critical pipes of water pipe networks for proactive seismic rehabilitation decision-making. Chapter 6 presents the conclusion of this study.

CHAPTER 2 : BACKGROUND

2.1. EXISTING SEISMIC VULNERABILITY ASSESSMENT MODELS

Component-level and system-level seismic vulnerability assessments are two broadly classified categories of methods for assessing the vulnerability of water pipe networks subjected to seismic events. Individual components can be evaluated by component-level assessment models. The seismic performance of an entire network can be evaluated by system-level assessment models. The methods for assessing the vulnerability of individual pipes can be further divided into two categories: analytical and empirical. Newmark and Rosenblueth (1971) proposed an analytical method to investigate the response of an underground pipeline assuming negligible soil-pipe interaction. Since then, these interactions have been studied using quasi-static analysis (Singhal and Zuroff 1990; Wang et al. 1982), shell theory (Liu et al. 2004; Luco and De Barros 1994), dynamic plain-strain modeling (Datta et al. 1984), finite element analysis (Saberli et al. 2014; Vazouras et al. 2010), probabilistic fault displacement hazard analysis and beam-type finite element modeling (Melissianos et al. 2016), and nonlinear modeling of seismic response (Hosseini and Tahamouli Roudsari 2010). Honegger and Eguchi (1992) estimated the failure rate of brittle pipes subjected to permanent ground deformation. American Lifeline Airlines (ALA 2001) formulated seismic fragility relations for a wide range of pipes based on 81 data points from 12 earthquakes. Although these component-level models are useful to gain a good insight into failure mechanisms of small-scale cases, they are impractical for large-scale vulnerability assessment (Hosseini and Tahamouli Roudsari 2010).

While it is necessary to understand the performance of individual pipes, their network resilience depends on these pipes' dynamic interactions. Advancements in network simulation, probabilistic modeling, and computational engineering have helped researchers to conduct system-level seismic vulnerability assessments of networks (Pudasaini et al. 2017; Wang et al. 2010; Shi 2006). Individual pipe failure probabilities are used to generate damage in pipes for system-level vulnerability assessment (Pudasaini and Shahandashti 2020b). Damages were integrated with hydraulic models using Monte Carlo simulation. Shi (2006) combined fragility relations with hydraulic principles to model the seismic response of water networks. Shi's methodology was further expanded to generate various system serviceability and reliability indices (Wang et al.

2010; Huang et al. 2008). System serviceability index (SSI) was used by Wang et al. (2010) to measure the performance of a water pipe network susceptible to seismic damages. SSI was used to locate the critical pipes of the network and rank them accordingly. Networks' spatial distributions and correlations related to ground motion intensities were not taken into consideration in their analysis.

Several seismic rehabilitation decision-making models have already been developed based on the existing seismic vulnerability assessment models. Pudasaini and Shahandashti (2018) developed a genetic algorithm-based optimization algorithm to develop a seismic rehabilitation decision-making model. Shahandashti and Pudasaini (2019) proposed a simulated annealing-based methodology to identify critical pipes of a water distribution network considering budget limitation, spatial correlation between seismic intensities, and the correlation between the effects of pipes' damages on the network serviceability. Roy et al. (2021) and Roy et al. (2022) identified the effects of network uncertainties on seismic vulnerability assessment of water distribution networks. Sharveen et al. (2022) developed a risk-based algorithm to identify critical pipes. Roy et al. (2023) investigated the effects of water network uncertainties on proactive seismic rehabilitation decision-making of water distribution networks.

2.2. EFFECT OF NETWORK UNCERTAINTIES ON DESIGN PHASE AND OPERATIONAL PHASE

Although the impacts of uncertainties on the seismic vulnerability assessments are unknown, uncertainty quantification and analysis have been applied to study the effects of water pipe network uncertainties on their no-hazard design and operation procedures. For example, Seifollahi-Aghmiuni et al. (2011) combined a shuffled frog algorithm with Monte Carlo simulation to examine water network efficiency considering the uncertainty of demand. Their study was primarily focused on identifying the effects of demand uncertainty on operation using a probabilistic normal distribution. They concluded that network efficiency decreases if demand uncertainty is not considered while operating a network. Seifollahi-Aghmiuni et al. (2013) used a similar methodology to examine water network performance in its operational period considering pipe roughness uncertainty. They concluded that if pipe roughness uncertainty increases, network

performance decreases. Xu and Goulter (1998) proposed a methodology for assessing water pipe networks considering uncertainties in pipe capacity, nodal demands, and reservoir/tank levels.

Lansey et al. (1989) developed a methodology to determine an optimal design process for water pipe networks. They considered several network uncertainties, such as pressure head requirements, future demands, and pipe roughness. They illustrated that uncertainties in those parameters have substantial effects on the network design process. Kapelan et al. (2005) defined the water distribution design problem as a multi-objective optimization problem under uncertainty. They considered pipe roughness coefficient and water consumption as uncertain variables. Probability density functions were used to model the uncertain variables. The obtained results demonstrated that the proposed methodology could identify robust Pareto optimal solutions in spite of the considerably less calculation effort. Sabzkouhi and Haghghi (2016) introduced a methodology to analyze water pipe networks considering uncertainty based on fuzzy set theory. They showed that uncertainties in network input parameters lead to imprecise hydraulic responses. Implementing the method in a real-time network revealed that a 15% change in the nodal demand and pipes' roughness could result in -41.7% to +50.1% uncertainty in the pipe velocities and -11.2% to +6.4% uncertainty in the nodal pressures.

2.3. EXISTING WATER PIPE DEGRADATION MODEL

Existing degradation models can be broadly classified into two major categories: deterministic model and probabilistic model.

Deterministic models can be further classified into two sections based on the type of equation to predict the degradation rate: exponential models (e.g., Shaban et al. 2023; Pouri and Heidarimozaffar 2022; Barton et al. 2022; Clark et al. 1982; Walski and Pelliccia 1982; Shamir and Howard 1979) and linear models (Jacobs and Karney 1994; Kettler and Goulter 1985; McMullen 1982). Deb (2002) used a deterministic model of water pipe degradation to identify optimal replacement strategy of a water distribution network. Farshad (2004) used a deterministic model of water pipe degradation to predict the service life of a water distribution network using basic regression and standard extrapolation method. Seica and Packer (2004) developed a method to determine the mechanical strength of pipes using finite element evaluation model of water pipe

degradation. Seica and Packer (2006) proposed a different method to predict the mechanical strength of pipes using a simplified numerical method of water pipe degradation.

The probabilistic models of water pipe degradation can be divided into five models: Bayesian diagnostic model (e.g., Watson et al. 2004), cohort survival model (e.g., Deb et al. 1998; Herz 1996), break clustering model (e.g., Goulter et al. 1993; Goulter and Kazemi 1988), Semi-Markov chain (e.g., Gustafson and Clancy 1999), and data filtering (e.g., Mavin 1996). Sadiq et al. (2004) developed a probabilistic approach to conduct risk analysis due to degradation associated failures in cast iron pipes. Davis et al. (2008) used a probabilistic approach of pipe degradation to predict the failure rate and scheduling of replacement for a water pipe network. Watson et al. (2004) identified maintenance scheduling using a Bayesian-based pipe degradation model. Christodoulou et al. (2003) used neuro-fuzzy systems and statistical modeling techniques to evaluate the structural degradation of the water distribution network in an urban setting. Al Barqawi and Zayed (2006) and Al Barqawi and Zawad (2008) used two different artificial neural network (ANN) based approaches of pipe degradation to predict ratings of pipelines. Punurai and Davis (2017) considered degradation to develop a prioritization technique using Monte Carlo simulation. Ji et al. (2017) developed an approach to model corroded cast iron pipes for lifetime prediction. Tavakoli et al. (2020) predicted useful remaining life of water pipe network using artificial neural networks and an adaptive neuro-fuzzy model of pipe degradation.

Degradation of pipe is also a function of pipe age (Annus and Vassiljev 2015; St. Clair and Sinha 2012). The age of the pipe has a direct effect on the hydraulic model and seismic fragility curves of the water pipe network. Extensive research has already been conducted that showed the effect of age on the pipe roughness coefficient (e.g., Herwig et al. 2008; Shin et al. 2016; Boxall et al. 2004; Sharp and Walski 1988; Mamrelli and Streicher 1962; Williams and Hazen 1960; Colebrook and White 1937a, b). Seismic fragility functions can also be affected due to the age of the pipes (Wang 1990; Eidinger 1998; Mazumder et al. 2019).

2.4. GAPS IN KNOWLEDGE

1. Existing methods for assessing the seismic vulnerability of water pipe networks did not consider the network uncertainties.

2. Existing seismic vulnerability assessment models and seismic rehabilitation decision-making models for water pipe networks do not consider the effects of degradation.

2.5. **RESEARCH OBJECTIVE**

1. Characterize and integrate the water pipe network uncertainties with a seismic vulnerability assessment model and identify the effects on the maximum serviceability of a water pipe network.
2. Identify the effects of network uncertainties on seismic rehabilitation decision-making of water pipe networks.
3. Identify the effects of water pipe on seismic rehabilitation decision-making of water pipe networks.

CHAPTER 3 : EFFECT OF NETWORK UNCERTAINTY ON SEISMIC VULNERABILITY ASSESSMENT OF WATER PIPE NETWORKS

Although existing seismic vulnerability assessment methods are sensitive to water pipe network uncertainties (e.g., uncertainties in nodal demand, reservoir head, pipe roughness coefficient), the extent of the effects of these uncertainties on post-earthquake serviceability of the networks has not been examined. This research investigates the effects of water pipe network uncertainties on the seismic vulnerability assessment of networks. The methodology includes seven steps: uncertainty identification and quantification, design of experiments, integrated multi-physics modeling, seismic repair rate calculations, Monte Carlo simulation, statistical analysis of the data (Analysis of Variance (ANOVA), and Tukey tests), and sensitivity analysis. Uncertainties in nodal demand, reservoir head, and pipe roughness coefficient were examined in this study. An integrated multi-physics model was created to simulate hydraulic network behavior and seismic vulnerability assessment. The approach was tested on two networks (New York Tunnel Network and Oberlin Network).

3.1. METHODOLOGY

The methodology includes seven steps: uncertainty identification and quantification, design of experiments, integrated multi-physics modeling, seismic repair rate calculations, Monte Carlo simulation, statistical analysis of the data (ANOVA test and Tukey Test), and sensitivity analysis. Figure 3.1 demonstrates the methodology adopted for this study.

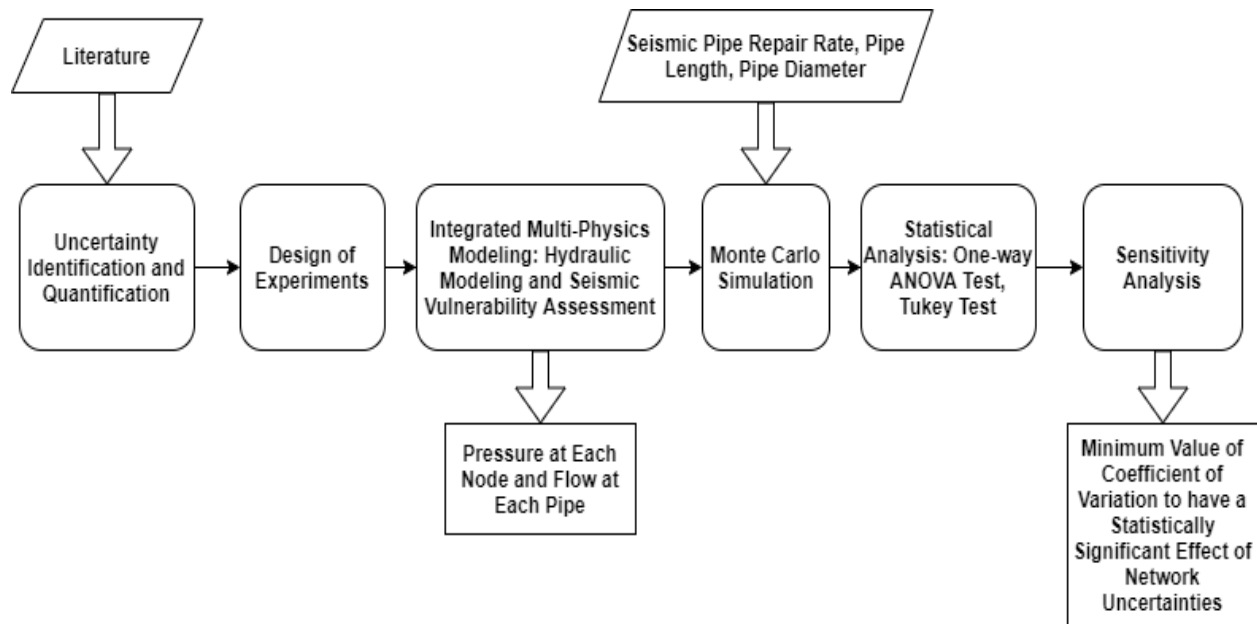


Figure 3.1: Methodology for investigating effects of network uncertainties

3.1.1. Uncertainty Identification and Quantification

Sources of water pipe network uncertainties were identified and quantified based on the literature. Probability and possibility models were used to characterize pipe network uncertainties. Table 3.1 summarizes the previous efforts to characterize the network uncertainties. Normal and uniform distributions were two widely used probability models (Seifollahi-Aghmiuni et al. 2013; Lansey et al. 2001). Alternatively, fuzzy logic was used as a possibility model (Sabzkouhi and Haghighi 2016; Shibu and Janga Reddy 2011).

Table 3.1: Water network uncertainty models in the literature

Parameters	Probability and Possibility Models	References
Pipe Roughness Coefficient	Normal Distribution	Seifollahi-Aghmiuni et al. (2013); Lansey et al. (2001); Xu and Goulter (1998); Lansey et al. (1989)
	Uniform Distribution	Kang and Lansey (2009); Kapelan et al. (2005); Xu and Goulter (1998)
	Fuzzy Numbers	Pandey et al. (2020); Dongre and Gupta (2017); Sivakumar et al. (2016); Sabzkouhi and Haghighi

		(2016); Haghghi and Asl (2014); Shibu and Janga Reddy (2011)
Nodal Demand	Normal Distribution	Seifollahi- Aghmiuni et al. (2013); Lansey et al. (2001); Xu and Goulter (1998); Lansey et al. (1989)
	Uniform Distribution	Kang and Lansey (2009)
	Fuzzy Numbers	Pandey et al. (2020); Dongre and Gupta (2017); Sivakumar et al. (2016); Sabzkouhi and Haghghi (2016); Haghghi and Asl (2014)
Reservoir Head	Normal Distribution	Xu and Goulter (1998)
	Fuzzy Numbers	Sabzkouhi and Haghghi (2016)
Pipe Materials	Uniform Distribution	Kang and Lansey (2009)
Age	Uniform Distribution	Kang and Lansey (2009)
	Fuzzy Numbers	Braun et al. (2020)
Diameter	Uniform Distribution	Kang and Lansey (2009)

Through a thorough literature review, three water pipe network uncertainties were selected: nodal demand, pipe roughness coefficient, and reservoir head. These uncertainties are widely acknowledged in the literature as critical sources of uncertainties for performance modeling and analysis of the water pipe networks (Table 3.1). It is assumed nodal demands, pipe roughness coefficient, and reservoir head to be normally distributed. The coefficient of variation (CoV) was used to investigate the effect of uncertainty. CoV is the ratio between the mean and standard deviation. The value of CoV was initially assumed to be 0.2 (Seifollahi-Aghmiuni et al. 2013). Later, different values of CoV were used to conduct the sensitivity analysis.

3.1.2. Design of Experiments

The experiments were designed as a full factorial design. Each of the three parameters considered in this study was studied at two levels: including uncertainty and excluding uncertainty. The levels were coded as +1 (including uncertainties) and -1 (excluding uncertainties). Table 3.2 shows selected water pipe network uncertainties with their levels for the experiment.

Table 3.2: Water pipe network uncertainties with their levels for the experiment

Name of water pipe network uncertainty	Notation of uncertainty	Levels	
		Including Uncertainty	Excluding Uncertainty
Nodal Demand	A	+1	-1
Pipe Roughness Coefficient	B	+1	-1
Reservoir Head	C	+1	-1

It is essential to analyze all the two-factor interactions to identify the effects of all three selected water pipe network uncertainties. Therefore, a 2^3 full factorial design was chosen for this experiment. The coded design for the experiment is shown in Table 3.3.

Table 3.3: Design matrix of the experiment

Experiment Name	Experiment Notation	A	B	C
Experiment 1	Com_Exp 1	-1	-1	-1
Experiment 2	Com_Exp 2	+1	-1	-1
Experiment 3	Com_Exp 3	-1	+1	-1
Experiment 4	Com_Exp 4	-1	-1	+1
Experiment 5	Com_Exp 5	+1	+1	-1
Experiment 6	Com_Exp 6	-1	+1	+1
Experiment 7	Com_Exp 7	+1	-1	+1
Experiment 8	Com_Exp 8	+1	+1	+1

3.1.3. Seismic Repair Rate Calculation

Figure 3.2 illustrates the steps to calculate the seismic repair rate for each pipe.

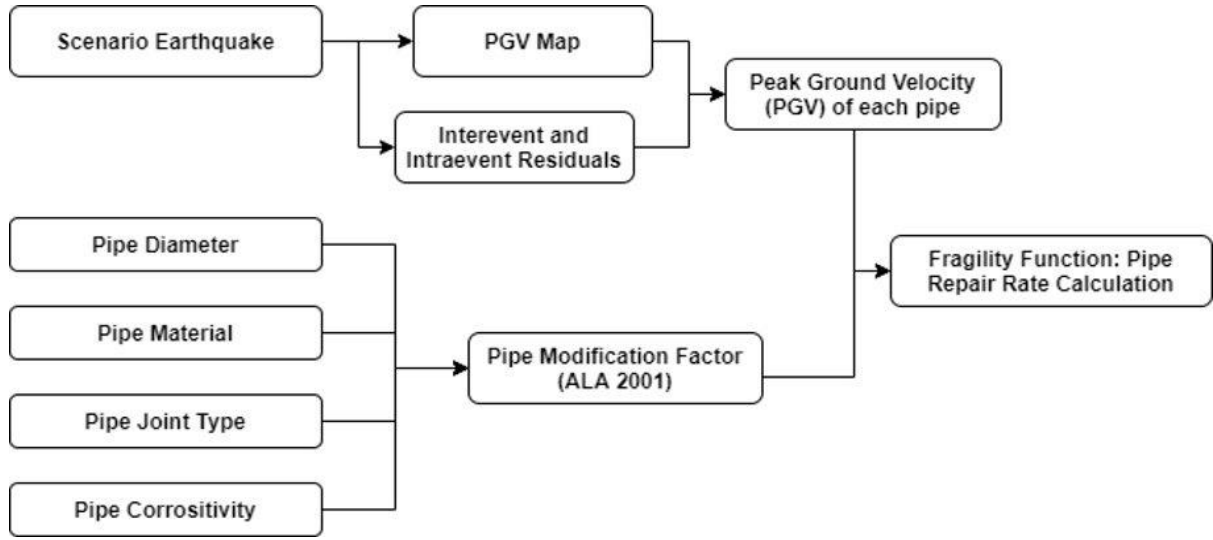


Figure 3.2: Steps of calculating seismic repair rate of each pipe

At the beginning of the seismic repair rate calculation, an earthquake scenario was identified based on deaggregation analysis using USGS (2018b) considering the spatial relationship among seismic intensities (Zanini et al. 2017; Zanini et al. 2016; Weatherill et al. 2013; Jayaram and Baker 2009; Adachi 2007). Deaggregation maps were generated using USGS (2018b). Deaggregation analysis was conducted using the spectral acceleration of 1.0-s. The earthquake that had the highest percentage of contribution was selected from the deaggregation analysis.

Next, for the selected earthquake scenario, peak ground velocity (PGV) was determined. PGV was used as the intensity parameter because of its direct relationship with the induced transient strains in the soil during a seismic event. These induced strains are major causes of underground pipe damage (Pineda-Porras and Najafi 2010).

A spatially correlated peak ground velocity field was produced using the ground motion prediction equation (GMPE) (Abrahamson and Silva 2007, Zanini et al. 2016, Zanini et al. 2017). The general equation is given by Eq. (3.1).

$$\log_{10}(PGV_{ab}) = f(M_a, R_{ab}, \theta_a) + \bar{\sigma}_B v_a + \bar{\sigma}_w \varepsilon_{ab} \quad (3.1)$$

where PGV_{ab} = value of peak ground velocity at location b from source a ; R_{ab} = distance between location a and location b ; M_a = earthquake magnitude; θ_a = fault geological parameters at location a . $\bar{\sigma}_B v_a$ is the interevent residual, and $\bar{\sigma}_w \varepsilon_{ab}$ is the intra-event residual. Initially, the peak ground velocity map, i.e., $f(M_a, R_{ab}, \theta_a)$ was created based on Abrahamson and Silva (2007). A peak

ground velocity map was created using the scenario shake map calculator (Field et al. 2005). In the following step, the interevent and intra-event variabilities were incorporated in this map. E_{ab} and v_a are random variables with normal distribution which has a mean value (K) of 0 and standard deviations of $\bar{\sigma}_B$ and $\bar{\sigma}_w$. The value of ε_{ab} was calculated using Eq. (3.2) (Zanini et al. 2016; Weatherill et al. 2013).

$$\varepsilon = K + Z * L \quad (3.2)$$

where $K = 0$; L = Lower triangular matrix; Z = vector of random variables with normal distribution. The value of L was calculated by applying the Cholesky decomposition method, such that $LL^T = P$. P is the positive-definite covariance matrix. The value of P can be calculated using Eq. (3.3).

$$P = \begin{bmatrix} 1 & \mathfrak{G}(d1,2) & \cdots & \mathfrak{G}(d1,N) \\ \vdots & 1 & \cdots & \mathfrak{G}(d2,N) \\ \vdots & \vdots & \ddots & \vdots \\ sym & \vdots & \cdots & 1 \end{bmatrix} \quad (3.3)$$

where $\mathfrak{G}(d a,b)$ is a correlation coefficient between intra-event residuals for location a and location b . N is the total number of locations. The value of $\mathfrak{G}(da,b)$ can be calculated using Eq. (3.4) (Jayaram and Baker 2009).

$$\mathfrak{G}(da,b) = e^{\left(\frac{-3da,b}{h}\right)} \quad (3.4)$$

where $d_{a,b}$ = distance between location a and location b . h is the intersite distance among which spatial relationships can be neglected. According to Wang and Takada (2005), when peak ground velocity is used to calculate spatial correlation, the value of h can be considered between 20 km to 40 km. For this study, the value of h was selected to be 30 km. This process was repeated for M times to create M random peak ground velocity fields (Zanini et al. 2017). The value of PGV for each pipe was calculated. Seismic pipe repair rates were then determined based on ALA (2001) using Eq. (3.5).

$$RR_{k,m} = C * 0.00187 * PGV_{k,m} \quad (3.5)$$

where $RR_{k,m}$ is the seismic repair rate per 1000 ft of pipe k for the m th seismic PGV field, C is the modification factor, and $PGV_{k,m}$ is the peak ground velocity at the location of pipe k for the m th seismic PGV field (in./s). The modification factor (C) adjusts the value of the repair rate considering the corrosivity of soil, pipe diameter, pipe material, and pipe joint characteristics.

3.1.4. Integrated Multi-physics Modeling and Monte Carlo Simulation

The System Serviceability Index (SSI) database was created using Monte Carlo simulation. SSI is a post-earthquake serviceability indicator that measures the serviceability of a water network after a seismic event. SSI is the ratio between demand fulfilled after a seismic incident and the total demand of the network at the regular operational period (Wang et al. 2010; Shi 2006). For this study, it was assumed that the demand is fulfilled at a node if the pressure at that node is more than a threshold pressure. Using the definitions, SSI is formulated as Eq. (3.6)

$$SSI = \frac{\sum_{n=1}^{TN} x_n * D_n}{\sum_{n=1}^{TN} D_n} \quad (3.6)$$

subject to

$$x_n = 1 \text{ if } P_n \geq P_{threshold}$$

$$x_n = 0 \text{ if } P_n < P_{threshold}$$

where SSI is the system serviceability index; D_n is the demand at node n ; TN is the nodes in the network; $P_{threshold}$ is the minimum pressure required at the node, which is selected by the demand for firefighting, and P_n is the pressure at node n . Hydraulic pressure of 20 psi (0.14 MPa) was used as the $P_{threshold}$ (Trautman et al. 2013).

Seismic damage (breaks and leaks) were modeled using the Poisson process. The location of the p^{th} damage (break or leak) in a pipe k was determined by Eq. (3.7).

$$l_{k,p} = l_{k,p-1} - \frac{1}{RR_{k,m}} * \ln(1 - Q1) \quad \text{where } l_{k,0} = 0 \quad (3.7)$$

where $l_{k,p}$ is the distance of p^{th} damage (break or leak) in pipe k from its start node, $RR_{k,m}$ is the seismic repair rate of pipe k , and $Q1$ is a uniformly distributed random number. The value of $Q1$ ranges from 0 to 1. If the distance of initial damage (break or leak), i.e., $l_{k,1}$ was less than the total length of pipe k , then another random number ($Q2$) between 0 and 1 was generated. The value of $Q2$ classifies the damage as either a leak or a break. If the value of $Q2$ was not more than 0.8, it was considered a leak; otherwise, it was considered a break (Shi 2006). The diameter of each leak was determined by further classifying those leaks based on Shi (2006). This process was repeated until the value of $l_{k,p}$ is more than the total length of the pipe.

After locating all the damages (breaks and leaks) and determining the diameters of all damages for each pipe of the network for the present Monte Carlo simulation, the damages (breaks and leaks) were combined into the hydraulic model of the original network. Pressure at each node (P_n) was determined. Pressure-driven steady-state hydraulic analysis was used to calculate the pressure at each node. The demand-driven analysis considers that the demand at every node is obtained, and this consideration is not a valid consideration for water networks disrupted by seismic events (Shi 2006; Cheung et al. 2005). To investigate the performance of actual networks after earthquakes, the following two assumptions are necessary according to Shi (2006):

- water demand at each node is not always obtained.
- nodes cannot have negative pressure.

For every run of the Monte Carlo simulation, the following steps were followed:

- 1) Analyzing hydraulic model of the network including seismic damages (breaks and leaks)
- 2) Removing any nodes having negative pressure
- 3) Step 1 and step 2 were repeated if there is any node with negative pressure.

Hydraulic pressure at each node (P_n) was calculated and recorded. SSI was calculated based on the demand at available nodes after removing all nodes with negative pressure for the predefined maximum Monte Carlo runs using Eq. (3.8):

$$SSI_r = \frac{1}{M} * \sum_{m=1}^M SSI_m \quad (3.8)$$

where SSI_r is the average value of SSI for r^{th} Monte Carlo simulation; SSI_m is the value of SSI calculated using Eq. (3.6) for the m^{th} PGV field; M is the total number of PGV fields generated for the selected earthquake scenario.

The value of SSI for each Monte Carlo run was then recorded to create the SSI database. The SSI database was used for statistical analysis (ANOVA test and Tukey test). The steps of the Monte Carlo simulation to create the database are shown in Figure 3.3.

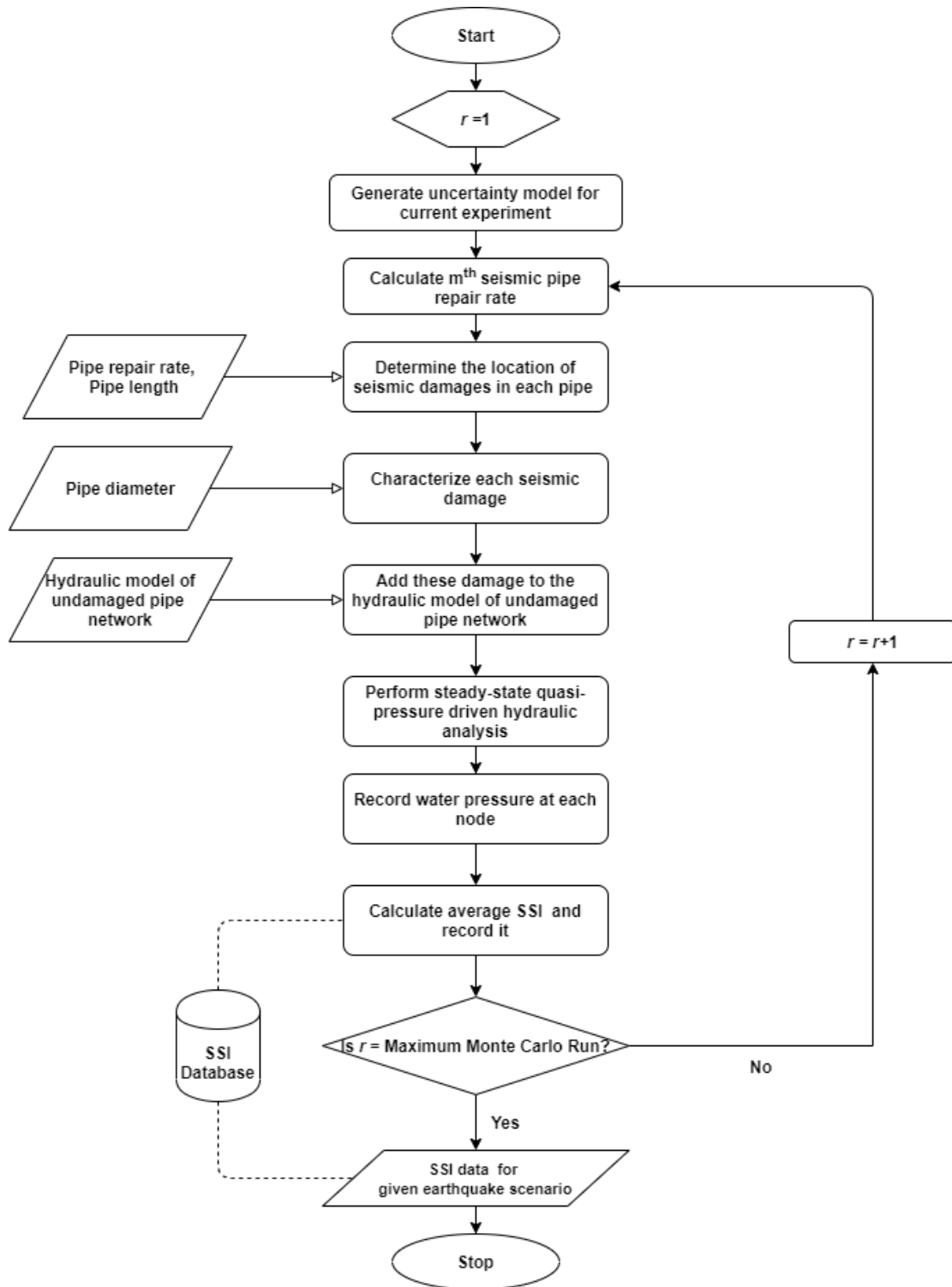


Figure 3.3: Steps of Monte Carlo simulation to create SSI database for each experiment for a given earthquake scenario for the m th PGV field

3.1.5. Statistical Analysis of the SSI Database

The one-way analysis of variance (ANOVA) and the Tukey test were used for statistical analysis of the SSI database. ANOVA is a statistical tool that determines any significant difference between the means of SSI of individual experiment groups. The following null hypothesis is tested:

$$H_0: \mu_1 = \mu_2 = \mu_3 = \dots = \mu_k \quad (3.9)$$

where μ is the mean of the individual experiment group, and k is the total number of individual experiment groups. If the result is significant from the ANOVA test, the null hypothesis is rejected, which implies that a minimum of two individual experiment groups are statistically different from each other.

The one-way ANOVA cannot determine which specific experiment groups are statistically different from each other. A Tukey test was performed to determine which particular groups differed from each other.

3.2. APPLICATION AND RESULTS

Two different networks were selected to demonstrate the application of the methodology. The first network was the New York Tunnel network (Water Distribution System Research Database), having 42 pipes, 19 junctions, and one reservoir. The second network was the Oberlin network (Water Distribution System Research Database), having 289 pipes, 262 junctions, and one reservoir. The Oberlin network is in Harrisburg, Pennsylvania.

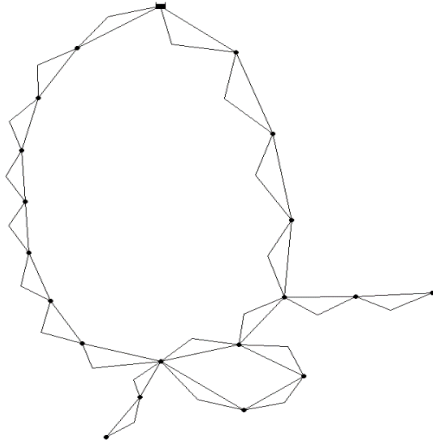


Figure 3.4: Layout of New York Tunnel network

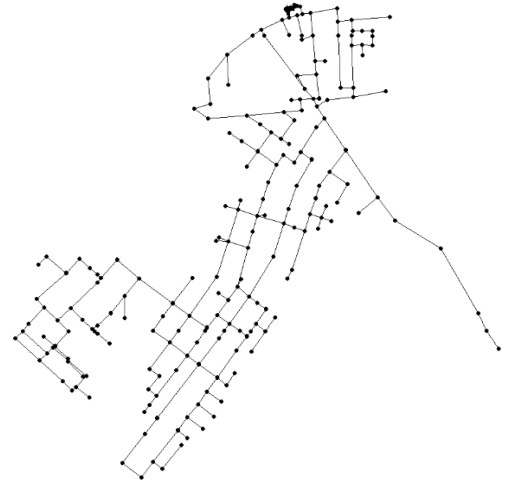


Figure 3.5: Layout of Oberlin network

The material of pipes having diameters less than 12 inches (300 mm) was assumed to be cast iron. The joint type for the cast-iron pipe was considered lead joints. If the diameter of the pipes were greater than 12 inches (300 mm), then the material was considered to be ductile iron. The joint type for the ductile iron pipe was considered rubber-gasketed joints.

To select an earthquake scenario to thoroughly analyze the impact of uncertainties on the seismic vulnerability assessment, networks' centroid was presumed to be in Pasadena, California (34.146267° N, 118.144040° W) for the deaggregation analysis. Deaggregation analysis was conducted using USGS (2018b). For the deaggregation analysis, the return period was selected to be 2,475 years. From the deaggregation results conducted in Pasadena, California, an earthquake at the Raymond fault was selected as the scenario earthquake (magnitude 7.13) for this study as it had the highest contribution ratio (13.96%).

In the following step, a peak ground velocity field was generated using scenario shake-map calculator (Abrahamson and Silva 2007; Field et al. 2005). Inter-event and intra-event residuals were not considered in the shake-map calculator. The generated peak ground velocity field is shown in Figure 3.6. Figure 3.7 shows the same peak ground velocity field magnified to the scale of the network for New York Tunnel network. Figure 3.8 shows the peak ground velocity field magnified to the scale of the network for Oberlin network.

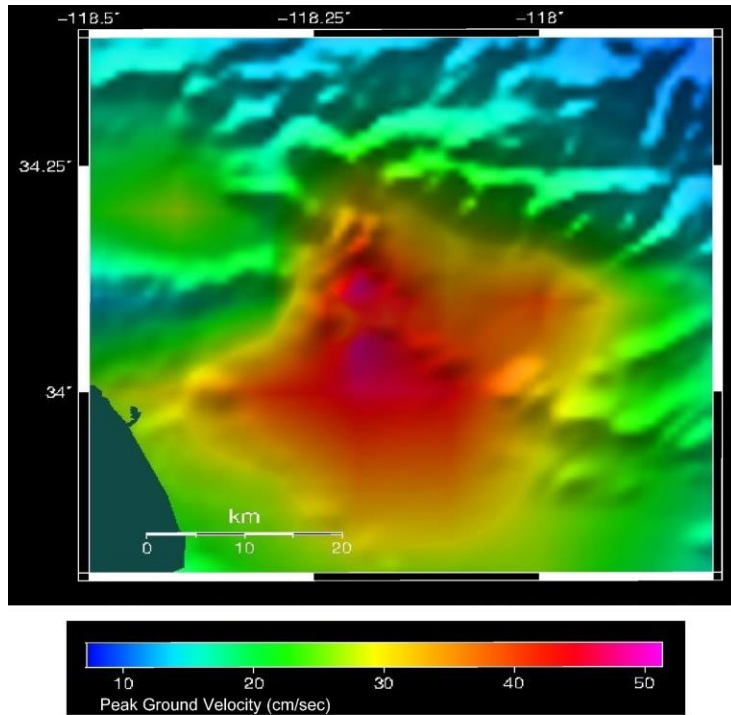


Figure 3.6: Peak ground velocity field due to the selected earthquake scenario without intraevent and interevent residuals

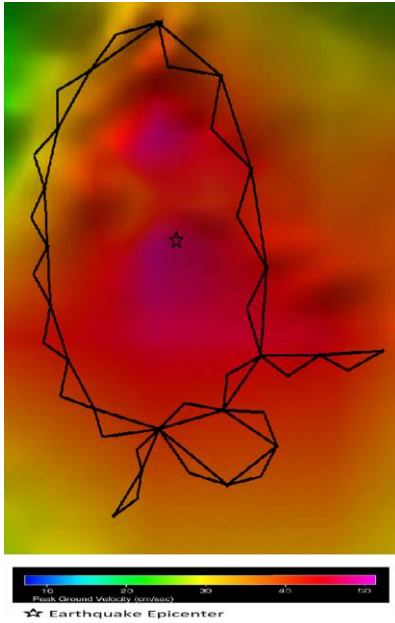


Figure 3.7: Peak ground velocity field due to the selected earthquake scenario without intraevent and interevent residuals zoomed to network scale for New York Tunnel network

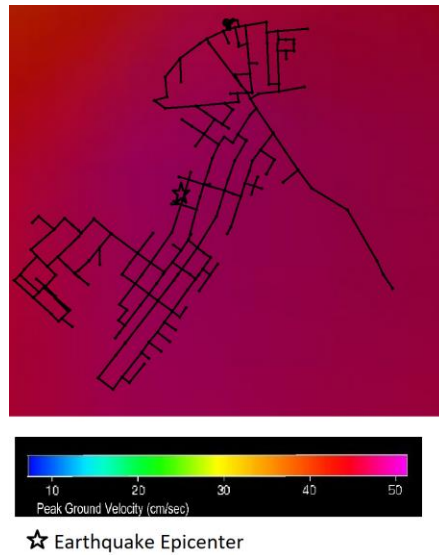


Figure 3.8: Peak ground velocity field due to the selected earthquake scenario without intraevent and interevent residuals zoomed to network scale for Oberlin network

Each junction and four equally spaced nodes along the length of each pipe were chosen to generate the intra-event and inter-event residuals. These residual vectors were combined with a peak ground velocity field to generate twenty random PGVs ($M=20$). The average PGV was quantified for each pipe using the PGV determined at the start junction of the pipe, at the end junction of the pipe, and four intermediate points along the pipe. The average PGV of each pipe was then used to measure the SSI of the network.

A convergence study was conducted to determine the suitable number of Monte Carlo runs (Figure 3.9). Oberlin network (Water Distribution System Operations) was selected to conduct the convergence study. Experiment 8, for the selected earthquake, was selected for the convergence study. The same number of Monte Carlo runs that was found from the convergence study was used both for both New York Tunnel network and the Oberlin network (Water Distribution System Operations). From the convergence study result shown in Figure 3.9, it was concluded that 3000 Monte Carlo runs were sufficient for this study.

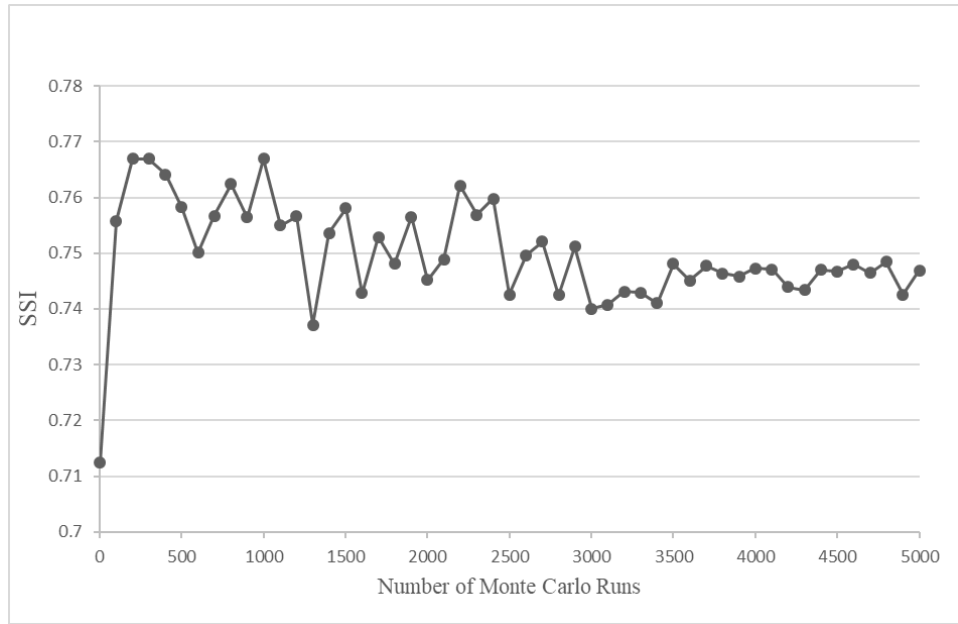


Figure 3.9: Convergence study using Oberlin network to identify sufficient Monte Carlo runs

A one-way ANOVA test was conducted (considering a 5% level of significance) to determine if the experimental results were statistically significant. Table 3.4 and Table 3.5 summarize the mean and variance of SSI for each experiment for the New York Tunnel network and Oberlin network, respectively.

Table 3.4: Mean and variance of SSI of each experiment for New York Tunnel network

Experiment Name	Average	Variance
Com_Exp 1	0.327	0.033
Com_Exp 2	0.323	0.031
Com_Exp 3	0.318	0.034
Com_Exp 4	0.405	0.024
Com_Exp 5	0.312	0.034
Com_Exp 6	0.407	0.023
Com_Exp 7	0.411	0.025
Com_Exp 8	0.408	0.024

Table 3.5: Mean and variance of SSI of each experiment for Oberlin network

Experiment Name	Average	Variance
Com_Exp 1	0.705	0.198
Com_Exp 2	0.708	0.197
Com_Exp 3	0.674	0.210
Com_Exp 4	0.755	0.139
Com_Exp 5	0.669	0.212
Com_Exp 6	0.750	0.138
Com_Exp 7	0.753	0.140
Com_Exp 8	0.748	0.141

For the ANOVA test, a null hypothesis (H_0) and an alternative hypothesis (H_1) were selected.

Null hypothesis, $H_0: \mu_1 = \mu_2 = \dots = \mu_8$

Alternative hypothesis, H_1 : Not all μ are equal.

Level of Significance: 5%

From the ANOVA test results, the p -values for New York Tunnel and Oberlin networks were much less than 0.05. Therefore, there were significant differences between the means of SSI in different groups or different experiments. The ANOVA test could not determine which specific experiments were statistically different from each other. It only implies that at least two experiments were statistically significant. The Tukey test that is often used for multiple pairwise comparisons was conducted to determine which experiments have significantly different means. As this study was only considering the effects of uncertainty, the Tukey test was conducted only for seven pairs, comparing no-uncertainty experiment (Com_Exp 1) with the other experiments: (Com_Exp 1, Com_Exp 2); (Com_Exp 1, Com_Exp 3); (Com_Exp 1, Cop_Exp 4); (Com_Exp 1, Com_Exp 5); (Com_Exp 1, Com_Exp 6); (Com_Exp 1, Com_Exp 7); (Com_Exp 1, Com_Exp 8). Table 3.6 and Table 3.7 summarize the results of the Tukey test for the New York Tunnel network and Oberlin network, respectively.

Table 3.6: Results of Tukey test for New York Tunnel network

Group 1	Group 2	meandiff	<i>p</i> -adj	Lower	Upper	Reject
Com_Exp 1	Com_Exp 2	-0.0035	0.9000	-0.0167	0.0097	FALSE
Com_Exp 1	Com_Exp 3	-0.0086	0.4942	-0.0219	0.0046	FALSE
Com_Exp 1	Com_Exp 4	0.0783	0.0010	0.0651	0.0916	TRUE
Com_Exp 1	Com_Exp 5	-0.0154	0.0099	-0.0286	-0.0022	TRUE
Com_Exp 1	Com_Exp 6	-0.0800	0.0010	0.0668	0.0933	TRUE
Com_Exp 1	Com_Exp 7	-0.0839	0.0010	0.0707	-0.0971	TRUE
Com_Exp 1	Com_Exp 8	-0.086	0.0010	0.0683	0.0948	TRUE

Table 3.7: Results of Tukey HSD test for Oberlin network

Group 1	Group 2	meandiff	<i>p</i> -adj	Lower	Upper	Reject
Com_Exp 1	Com_Exp 2	0.0029	0.9000	-0.0295	0.0353	FALSE
Com_Exp 1	Com_Exp 3	-0.0311	0.0717	-0.0635	0.0013	FALSE
Com_Exp 1	Com_Exp 4	0.0499	0.0010	0.0174	0.0823	TRUE
Com_Exp 1	Com_Exp 5	-0.0365	0.0152	-0.0689	-0.0040	TRUE
Com_Exp 1	Com_Exp 6	0.0454	0.0010	0.0129	0.0778	TRUE
Com_Exp 1	Com_Exp 7	0.0476	0.0010	0.0152	-0.0801	TRUE
Com_Exp 1	Com_Exp 8	0.0432	0.0014	0.0108	0.0757	TRUE

The Tukey test results of both the New York Tunnel network and Oberlin network show that demand uncertainty (Com_Exp 2) and pipe roughness coefficient uncertainty (Com_Exp 3) do not have statistically significant individual effects; the null hypothesis could not be rejected. For all other pairwise comparisons, the null hypothesis was rejected, and it was concluded that the effects of uncertainty are significant considering a 5% level of significance.

From the ANOVA and Tukey test results, it can be concluded that uncertainty of demand and pipe roughness coefficient uncertainty do not have statistically significant effects. On the other hand, the effects of reservoir head uncertainty are statistically significant. The combined effect of the three selected water pipe network uncertainties is statistically significant for the selected value of

CoV. In the next part of the study, sensitivity analysis was conducted to find the minimum value of CoV to create a statistically significant effect.

3.3. SENSITIVITY ANALYSIS

Sensitivity analysis was conducted to find the minimum value of the coefficient of variation (CoV) for which water pipe network uncertainties were statistically significant. Sensitivity analysis was divided into three major parts based on the effect of water pipe network uncertainties:

- (i) Effect of uncertainties in demand, pipe roughness coefficient, and reservoir head individually
- (ii) Combined effects of uncertainties in
 - (a) demand and pipe roughness coefficient.
 - (b) pipe roughness coefficient and reservoir head.
 - (c) demand and reservoir head
- (iii) Combined effect of uncertainties in demand, reservoir head, and pipe roughness coefficient

3.3.1. Effect of Individual Water Pipe Network Uncertainties

All three water pipe network uncertainties were studied individually for both networks. The results for both the networks are shown graphically in Table 3.8.

Table 3.8: Minimum value of CoV for each network uncertainties

Network Name: New York Tunnel Network	
Network Uncertainty	Minimum Value of CoV
Demand	1.00
Pipe Roughness Coefficient	0.40
Reservoir Head	0.01
Network Name: Oberlin Network	
Network Uncertainty	Minimum Value of CoV
Demand	0.50
Pipe Roughness Coefficient	0.30
Reservoir Head	0.01

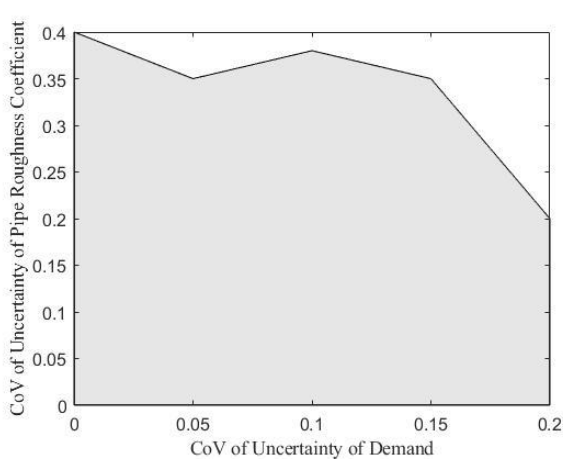
From the sensitivity test result of both the networks, the minimum value of CoV for reservoir head uncertainty is 0.01, indicating that a small uncertainty in reservoir head results in a statistically significant SSI change in both networks. By contrast, the CoV value for uncertainties in nodal demand and pipe roughness has to be quite large, more than the 0.2 value assumed in the literature (Seifollahi-Aghmiuni et al. 2013), to significantly affect mean SSI.

3.3.2. Joint Effect of Water Pipe Network Uncertainties

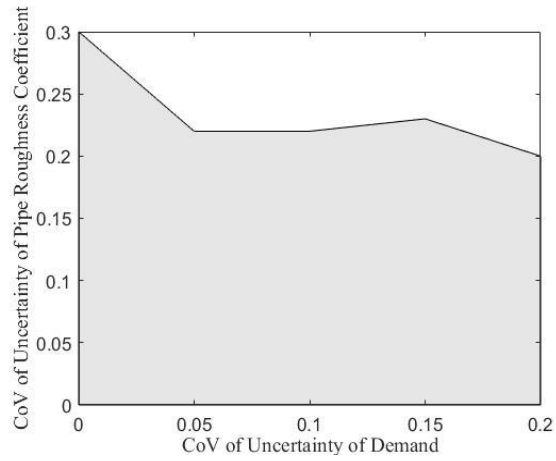
Two water pipe network uncertainties were considered together here:

- (i) Joint effect of uncertainties in demand and pipe roughness coefficient
- (ii) Joint effect of uncertainties in pipe roughness coefficient and reservoir head
- (iii) Joint effect of uncertainties in demand and reservoir head

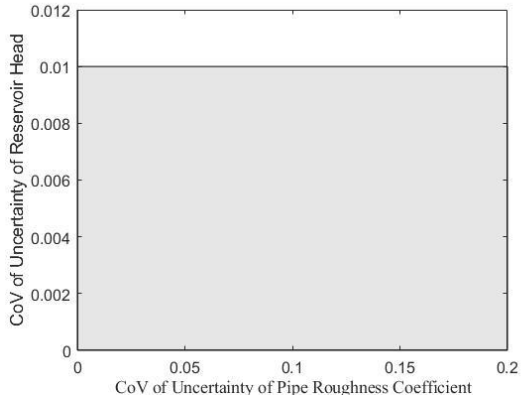
The analysis result of all three sections for both the networks are shown graphically from Figure 3.10(a) to Figure 3.10(f). The marked zone indicates the area inside which the joint effect of the water pipe network uncertainties is not statistically significant.



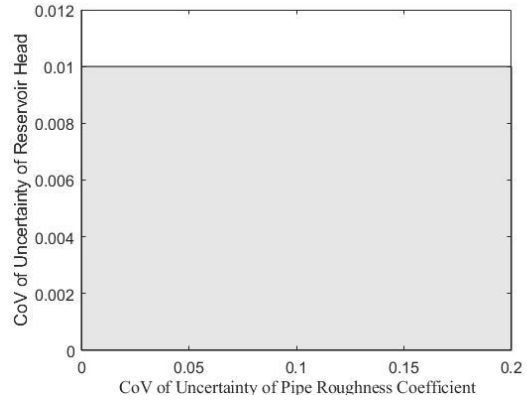
(a)



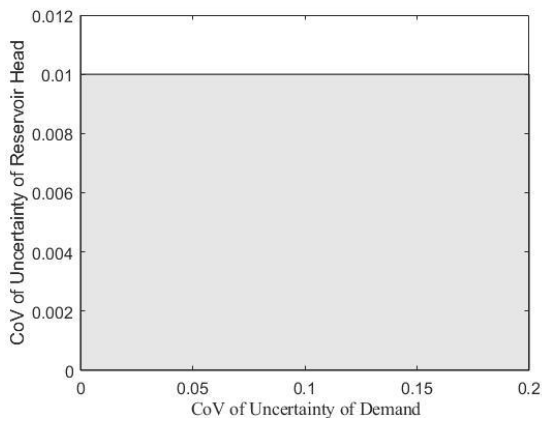
(b)



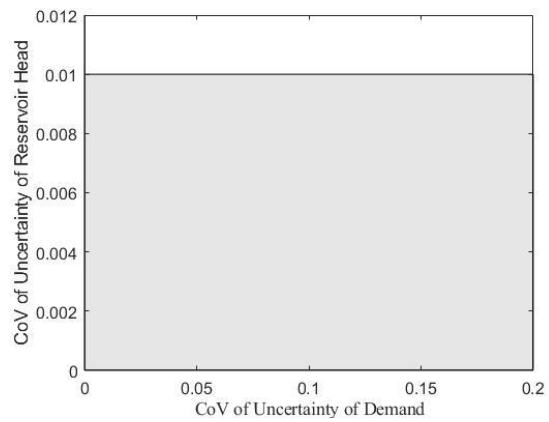
(c)



(d)



(e)



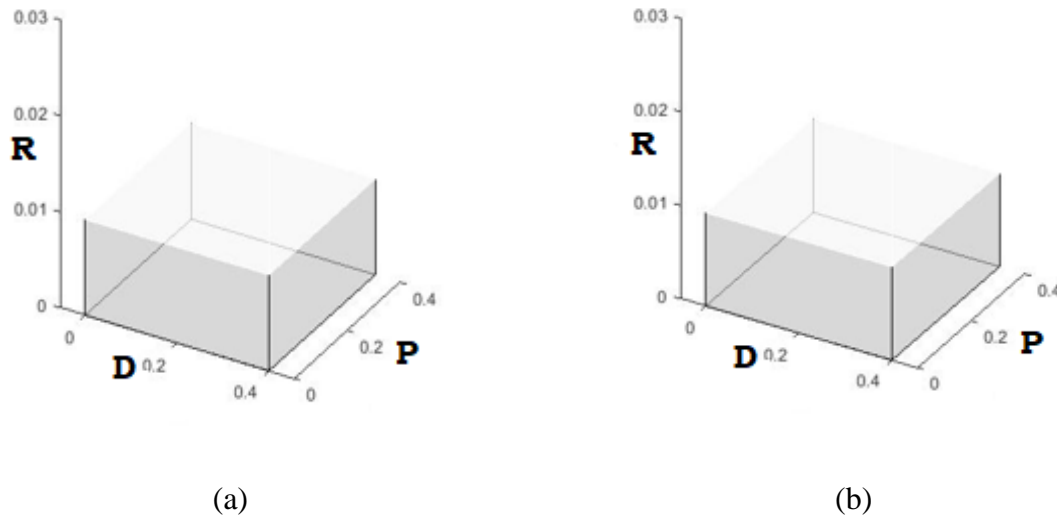
(f)

Figure 3.10: Result of sensitivity analysis with two water pipe network uncertainties (a) demand and pipe roughness coefficient for New York Tunnel network (b) demand and pipe roughness coefficient for Oberlin network (c) pipe roughness coefficient and reservoir head

Figure 3.10(a) and Figure 3.10(b) show that the minimum value of CoV for either uncertainty of demand or uncertainty of pipe roughness coefficient has to be high to result in a statistically significant change in SSI for both networks. By contrast, while checking the combined effects with reservoir head, the minimum value of CoV does not depend on the pipe roughness coefficient or demand to result in statistically significant SSI change for both networks as the value of SSI changes for any uncertainty in reservoir head.

3.3.3. Combined Effect of Three Water Pipe Network Uncertainties

All three water pipe network uncertainties were considered here. The results of the sensitivity analysis for both the networks are shown in Figure 3.11(a) and Figure 3.11(b). The marked zone indicates the zone inside which the combined effect of the water pipe network uncertainties is not statistically significant.



D = CoV of uncertainty of demand; P = CoV of uncertainty of pipe roughness coefficient; R = CoV of uncertainty of reservoir head

Figure 3.11: Result of sensitivity analysis with three water pipe network uncertainties (a) New York Tunnel network (b) Oberlin network

Figure 3.11(a) and Figure 3.11(b) show that the minimum value of CoV to have a statistically significant effect on the value of SSI does not depend on the uncertainty of demand and pipe roughness coefficient. A small uncertainty in reservoir head results in a statistically significant change in SSI for both networks.

3.4. DISCUSSION

Water pipe network hydraulic parameters are uncertain and probabilistic in nature. The probabilistic nature of network hydraulic parameters has a significant impact on hydraulic modeling of water pipe networks. Proactive seismic rehabilitation decision-making models are dependent on network hydraulic parameters. A methodology has been developed to integrate

uncertainties of network hydraulic parameters with existing network seismic vulnerability assessment methods and identify the effects of water pipe network uncertainties on seismic vulnerability assessment of networks. Three water pipe network hydraulic parameters were selected: uncertainties in nodal demand, reservoir head, pipe roughness coefficient. These selected parameters were considered probabilistic in nature with a fixed value of coefficient of variation. Two different networks were used to apply the proposed methodology.

The statistical analysis results show that the individual effect of probabilistic demand uncertainty and uncertainty of pipe roughness coefficient does not have a statistically significant effect. On the contrary, the individual effect of probabilistic reservoir head uncertainty is statistically significant. The statistical analysis results show that the joint effects these uncertainties (joint effect of uncertainty of demand and pipe roughness coefficient; joint effect of uncertainty of pipe roughness coefficient and reservoir head; joint effect of uncertainty of demand and reservoir head) are statistically significant. The combined effect of all three uncertain network parameters is statistically significant. An additional study was conducted to identify the minimum value of CoV to have a statistically significant impact on post-earthquake serviceability index for these three selected network hydraulic parameters.

CHAPTER 4 : IMPACT OF WATER NETWORK UNCERTAINTIES ON SEISMIC REHABILITATION DECISION-MAKING FOR WATER PIPELINES

Although water pipe network uncertainties play a critical role in seismic vulnerability assessment methods, the impacts of these uncertainties have not been explored in optimal proactive seismic rehabilitation decision-making. Extant pertinent literature ignores the uncertainty related to water network properties. This research aims to explore the impacts of water network uncertainties on determining the most critical pipes vulnerable to seismic events within a limited budget constraint. Pipe roughness coefficient, demand, and reservoir head were selected as uncertain network parameters for this study. Sensitivity analysis was performed to quantify selected network uncertainties. A stochastic combinatorial optimization problem was formulated considering network uncertainties and seismic ground motion intensities to identify the most critical pipes of a network for limited rehabilitation budget. A simulated-annealing algorithm was used to solve the stochastic combinatorial optimization problem. Modena network was used to demonstrate the method.

4.1. METHODOLOGY

The methodology for exploring the impacts of water network uncertainties on optimal seismic rehabilitation decision-making is described in Figure 4.1.

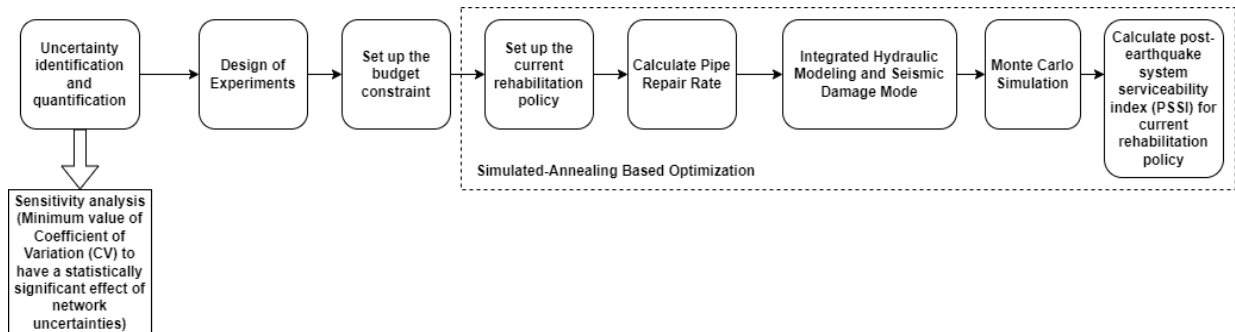


Figure 4.1: Methodology of exploring the impacts of water network uncertainties on optimal seismic rehabilitation decision-making

4.1.1. Selection of Network

The Modena network was used in this study (Center of Water Systems 2018). Modena network is a benchmark network with 268 junctions, 317 pipes, and 4 reservoirs. The total length of the pipes of the entire network is 71,806.11 m. For the calculation of seismic repair rate, pipes with diameters less than 300 mm (12 in.) were considered as cast-iron pipes with lead joints, whereas pipes with diameters greater than 300 mm (12 in.) were considered as ductile iron pipes with rubber-gasketed joints. Figure 4.2 shows the layout of the Modena network.

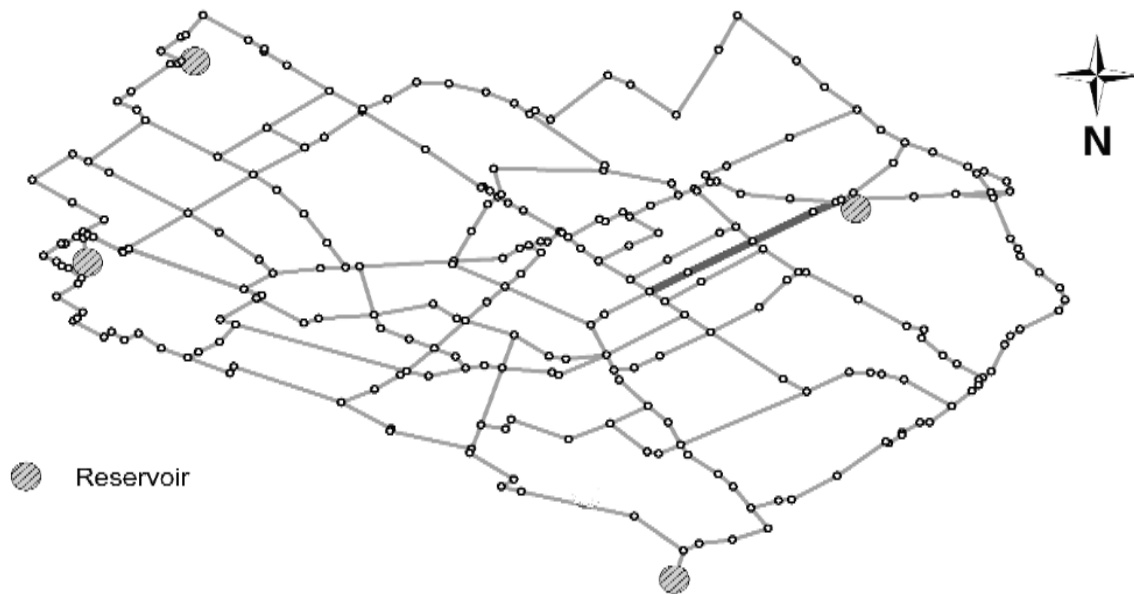


Figure 4.2: Layout of Modena network

4.1.2. Uncertainty Quantification

Three water network parameters were selected for this study: pipe roughness coefficient, nodal demand, and reservoir head. The probabilistic distribution for these parameters was assumed- 'Normal distribution'. CV was used as the parameter to quantify the uncertainties in this study (Roy et al. 2021). The minimum value of CV was used in this study. The minimum value of CV was determined using sensitivity analysis. Using the minimum value of CV ensures the integration of network uncertainty with the optimization algorithm. This study could have been conducted using a fixed value of CV (Roy et al. 2021). Selecting the fixed value of CV is not feasible for the optimization problem as there are chances of no effects for the predefined value of CV. The selected values of CV for all three uncertain parameters are listed in Table 4.1.

Table 4.1: Sensitivity analysis result

Network Uncertainty Parameter	Minimum Value of CV
Pipe Roughness Coefficient	0.15
Demand	0.50
Reservoir Head	0.10

4.1.3. Design of Experiments

To explore the effects of network uncertainty on optimal proactive seismic rehabilitation decision-making, this study was constructed as a full factorial design. All three selected network parameters were studied at two levels: uncertainty included (coded as 1) and uncertainty excluded (coded as -1) (Roy et al 2021). Table 4.2 shows the design of experiments for this study.

Table 4.2: Name of the experiments along with design matrix

Experiment Name/Notation	Pipe Roughness Coefficient	Demand	Reservoir Head
Exp A	-1	-1	-1
Exp B	-1	1	-1
Exp C	1	-1	-1
Exp D	-1	-1	1
Exp E	1	1	-1
Exp F	1	-1	1
Exp G	-1	1	1
Exp H	1	1	1

4.1.4. Calculating PSSI for Each Random PGV Field

Post-earthquake system serviceability index (PSSI) is used as a serviceability measure for this study (Wang 2010; Shi 2006). The same methodology described in section 3.1.3 and 3.1.4 was used to calculate the seismic repair rate of each pipe. After calculating the repair rate of each pipe,

PSSI was calculated for each random PGV (Shahandashti and Pudasaini 2019). The generated peak ground velocity field is shown in Figure 4.3. Figure 4.4 shows the same peak ground velocity field magnified to the scale of the network for Modena network.

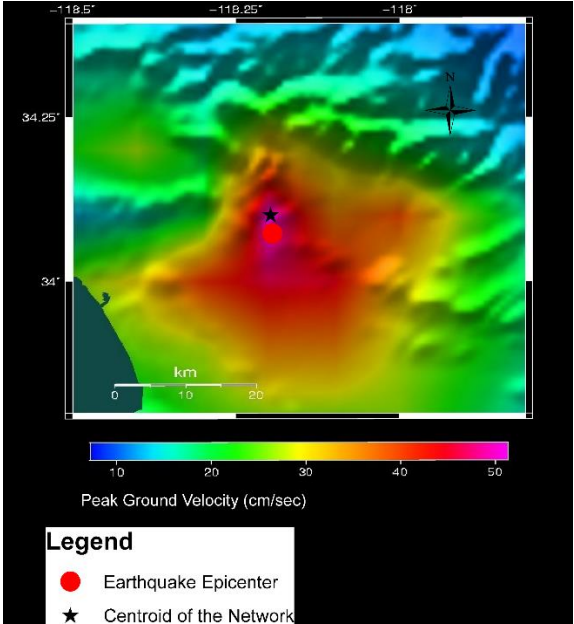


Figure 4.3: Peak ground velocity field due to the selected earthquake scenario without intraevent and interevent residuals

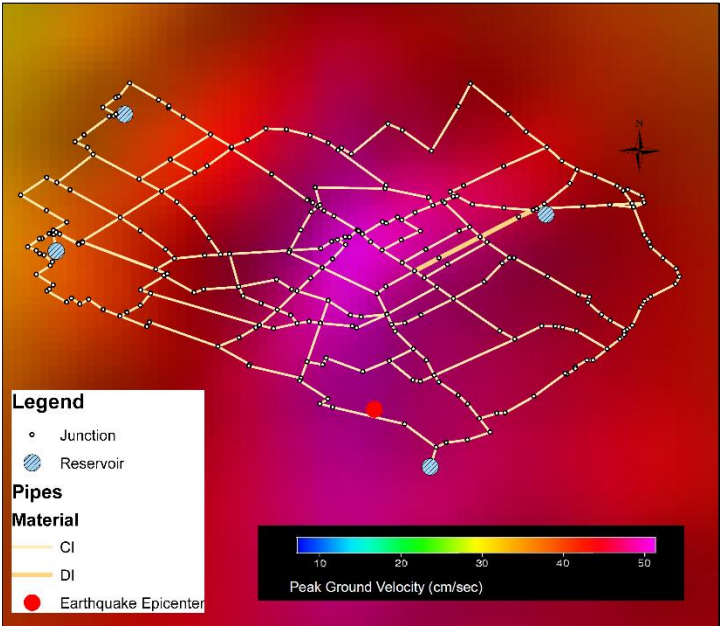


Figure 4.4: Peak ground velocity field due to the selected earthquake scenario without intraevent and interevent residuals zoomed to network scale for Modena network

4.1.5. Determining a Sufficient Number of Monte Carlo Runs

A sufficient number of Monte Carlo runs was identified based on a convergence study (Figure 4.5). From the convergence study, 3000 Monte Carlo runs were selected for this analysis.

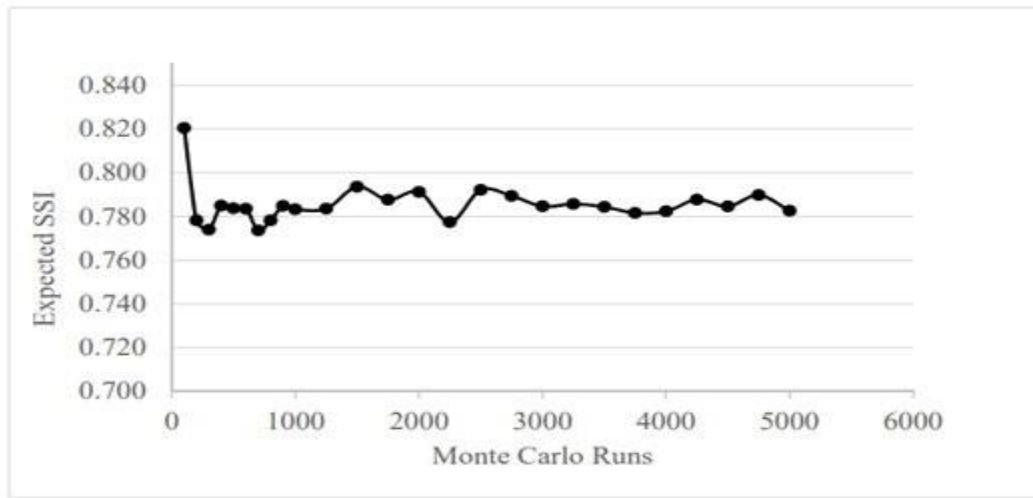


Figure 4.5: Result of convergence study

4.1.6. Optimization Problem Formulation

The problem targets maximizing the expected PSSI. The mathematical model can be represented by Eq. (4.1).

$$\max_{x \in X} E[PSSI(x)] \quad (4.1)$$

Subject to

$$Cost(x) \leq Cost_{max} \quad (4.2)$$

where all rehabilitation policies are denoted by set X, and $Cost(x)$ is the cost of rehabilitation to implement policy x , $Cost_{max}$ is the budget.

The combinatorial stochastic optimization problem was solved using a simulated-annealing-based optimization algorithm (Shahandashti and Pudasaini 2019). This study was conducted for five cost limits: \$2.5 million, \$5 million, \$7.5 million, and \$10 million. One method to ensure this is to replace the critical pipes with earthquake-resistant ductile iron (DI) pipes. These pipes have no record of any leaks and breaks in some major earthquakes in Japan in which almost all other utilities and infrastructures were severely affected (Haddaway 2015). Therefore, for this study, the critical pipes were assumed to be replaced with earthquake resistant pipes during seismic

rehabilitation of the pipe network. The cost data used for the rehabilitation are summarized in Table 4.3. The material costs and bare costs for installing ductile iron pipes manufactured in United States were obtained from RSMeans (2017). The backfill cost was obtained from JM Eagle (2017). These costs were added to get the total cost for installing ductile pipes manufactured in United States. Then the cost of installing earthquake-resistant Japanese ductile iron pipe was obtained by adjusting the price of US-manufactured pipe. The adjustment was based on the fact that the earthquake-resistant Japanese ductile iron pipe can be 3 times the price of US-manufactured ductile iron pipes (Haddaway 2015). The information regarding the earthquake resistant pipes' readily available diameters was obtained via correspondence with one of the major manufacturers of the pipes to formulate a practical rehabilitation policy. Using the created approach and the normalized cost vector (last column of Table 4.3), rehabilitation policies were identified for different rehabilitation budget constraints for the Modena network.

Table 4.3: Rehabilitation costs adopted for this study

Pipe diameter (mm)	US-manufactured ductile iron pipe				Earthquake-resistant Japanese ductile iron pipe		
	Material cost ^a (USD)	Bare cost without backfill cost ^a (USD)	Backfill cost ^b (USD)	Total cost with backfill cost (USD)	Bare cost without backfill cost ^c (USD)	Total cost with backfill cost (USD)	Normalized cost terms of 101.6-mm diameter pipe
101.60	30.50	42.58	4.49	47.07	103.58	108.07	1.00
152.40	26.50	41.57	5.15	46.72	94.57	99.72	0.92
203.20	44.50	62.62	5.83	68.45	151.62	157.45	1.46
254.00	58.50	79.61	6.50	86.11	196.61	203.11	1.88
304.80	79.00	101.94	7.20	109.14	259.94	267.14	2.47
355.60	93.00	117.16	7.91	125.07	303.16	311.07	2.88
406.40	94.50	127.50	8.63	136.13	316.50	325.13	3.01
457.20	126.00	160.80	9.37	170.17	412.80	422.17	3.91
508.00	127.00	169.10	10.12	179.22	423.10	433.22	4.01
609.60	141.00	192.25	11.66	203.91	474.25	485.91	4.50

^a Based on RSMeans (2017) data for Class 50 water piping with 5.4864-m (18-ft.) length.

^b Based on JM Eagle (2017). Backfill is assumed to be 30.48 cm (1 ft) above the top of the pipe, the backfill cost is assumed to be \$0.015/kg, and the density of the backfill is assumed to be 2,162.49 kg/m³ (135 lb/ft³).

^c Assumes that material cost of Kubota-manufactured earthquake-resistant DI pipes is 3 times the cost of DI pipes manufactured in the US based on Haddaway (2015).

4.2. RESULTS AND DISCUSSION

In the following section, the result from the simulated-annealing based optimization is demonstrated. Tables 4.4 to 4.7 show the maximum expected PSSI and actual cost of rehabilitation for different experiments of this study. Figure 4.6 to Figure 4.9 display the most critical pipes for each experiment considering the budget limitation. The actual cost was calculated based on the cost of rehabilitation for each pipe (Shahandashti and Pudasaini 2019). The critical pipes are highlighted using bold red marks.

Table 4.4: Maximum expected PSSI and actual cost of rehabilitation (Budget \$2.5 million)

Experiment Name	Actual Cost (USD)	Expected PSSI	Solution Time (h)
Exp A	2,446,678.00	0.891	301.5
Exp B	2,424,668.00	0.878	311.0
Exp C	2,463,208.00	0.875	302.0
Exp D	2,456,355.00	0.879	291.5
Exp E	2,425,674.00	0.866	308.0
Exp F	2,486,782.00	0.868	312.0
Exp G	2,410,406.00	0.872	302.5
Exp H	2,494,608.00	0.855	307.0

Table 4.4 indicates that the value of maximum expected PSSI decreases by 2% for consideration of single uncertain parameter, while this value reduces by 3% for consideration of two uncertain parameters combinedly. The maximum expected PSSI decreases by 4%, if we consider three uncertain parameters (Exp H)

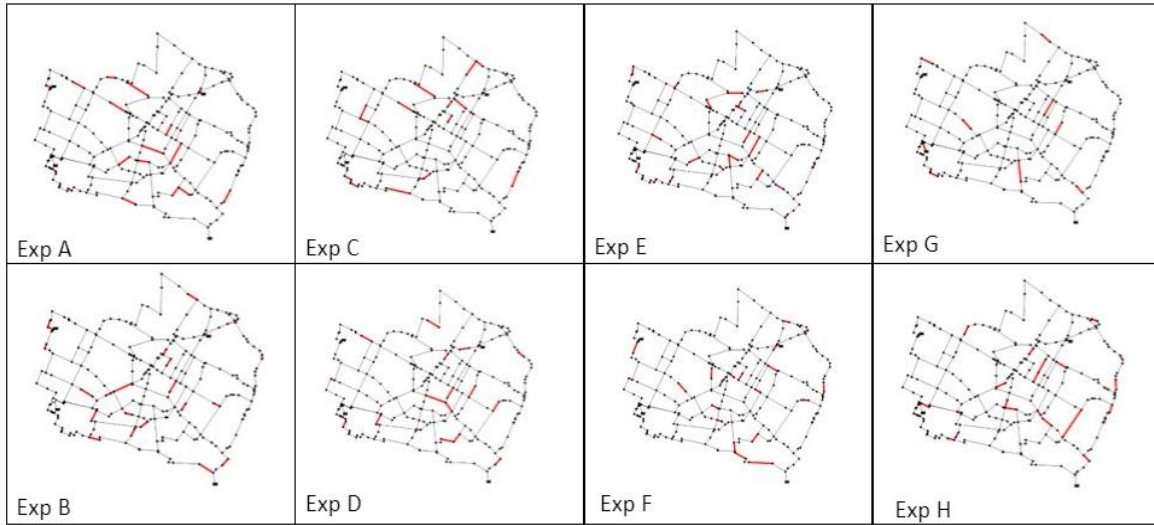


Figure 4.6: Critical pipes identified for different experiments (Budget \$2.5 million)

Table 4.5: Maximum expected SSI and actual cost of rehabilitation (Budget \$5 million)

Experiment Name	Actual Cost (USD)	Expected PSSI	Solution Time (h)
Exp A	4,934,951.00	0.903	292.5
Exp B	4,950,760.00	0.897	320.0
Exp C	4,944,896.00	0.892	322.0
Exp D	4,964,729.00	0.900	315.5
Exp E	4,984,016.00	0.883	303.0
Exp F	4,969,680.00	0.886	294.5
Exp G	4,981,897.00	0.889	294.5
Exp H	4,993,186.00	0.877	312.45

Table 4.5 indicates that the value of maximum expected PSSI decreases by 1% for consideration of single uncertain parameter, while this value reduces by 2% for consideration of two uncertain parameters combinedly. The maximum expected PSSI decreases by 3%, if we consider three uncertain parameters (Exp H).

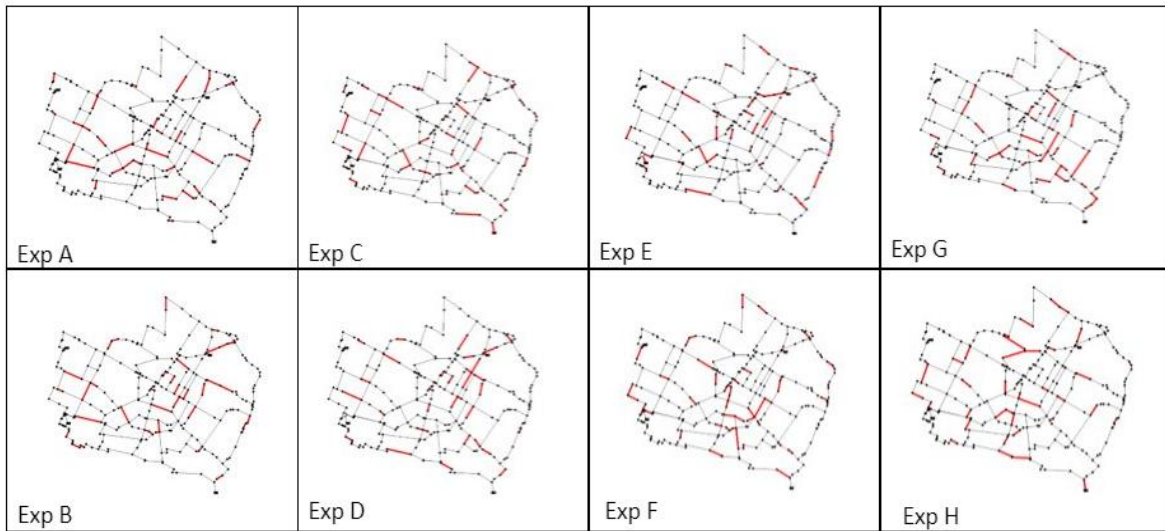


Figure 4.7: Critical pipes identified for different experiments (Budget \$5 million)

Table 4.6: Maximum expected SSI and actual cost of rehabilitation (Budget \$7.5 million)

Experiment Name	Actual Cost (USD)	Expected PSSI	Solution Time (h)
Exp A	7,459,747.00	0.921	283.0
Exp B	7,427,873.00	0.915	293.0
Exp C	7,499,606.00	0.916	289.0
Exp D	7,409,873.00	0.914	282.5
Exp E	7,484,499.00	0.905	293.5
Exp F	7,461,260.00	0.907	294.5
Exp G	7,453,703.00	0.906	299.0
Exp H	7,472,017.00	0.894	294.5

Table 4.6 indicates that the value of maximum expected PSSI decreases by 1% for consideration of single uncertain parameter, while this value reduces by 2% for consideration of two uncertain

parameters combinedly. The maximum expected PSSI decreases by 3%, if we consider three uncertain parameters (Exp H)

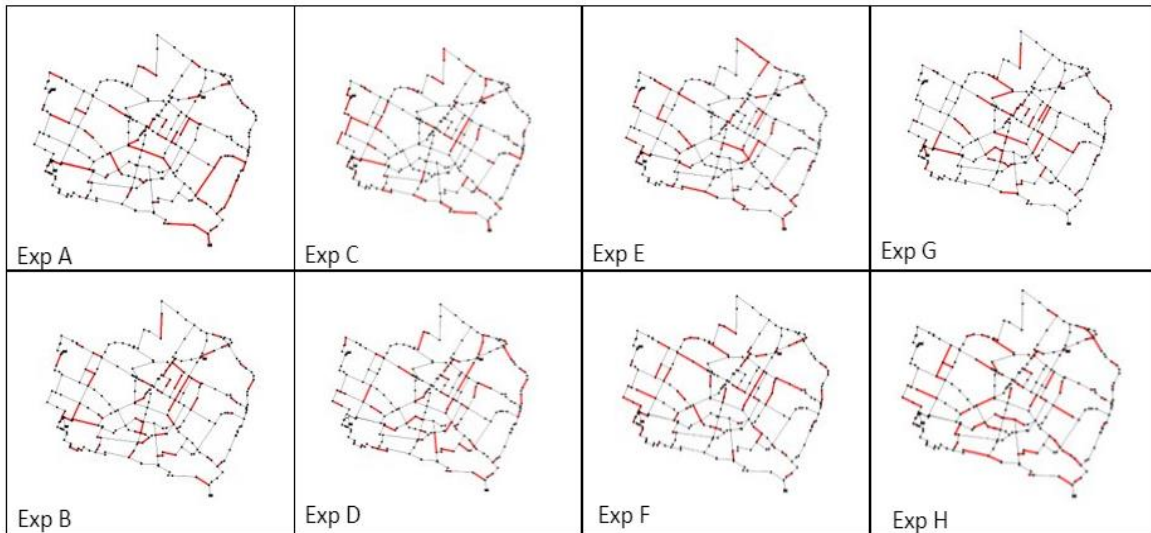


Figure 4.8: Critical pipes identified for different experiments (Budget \$7.5 million)

Table 4.7: Maximum expected SSI and actual cost of rehabilitation (Budget \$10 million)

Experiment Name	Actual Cost (USD)	Expected PSSI	Solution Time (h)
Exp A	9,907,578.00	0.940	279.0
Exp B	9,954,539.00	0.934	285.0
Exp C	9,966,649.00	0.932	282.0
Exp D	9,983,350.00	0.935	281.5
Exp E	9,930,516.00	0.924	296.0
Exp F	9,944,433.00	0.927	281.0
Exp G	9,988,639.00	0.926	287.0
Exp H	9,851,909.00	0.918	300.0

Table 4.7 indicates that the value of maximum expected PSSI remains same for consideration of single uncertain parameter, while this value reduces by 1% for consideration of two uncertain parameters combinedly. The maximum expected PSSI decreases by 3%, if we consider three uncertain parameters (Exp H)

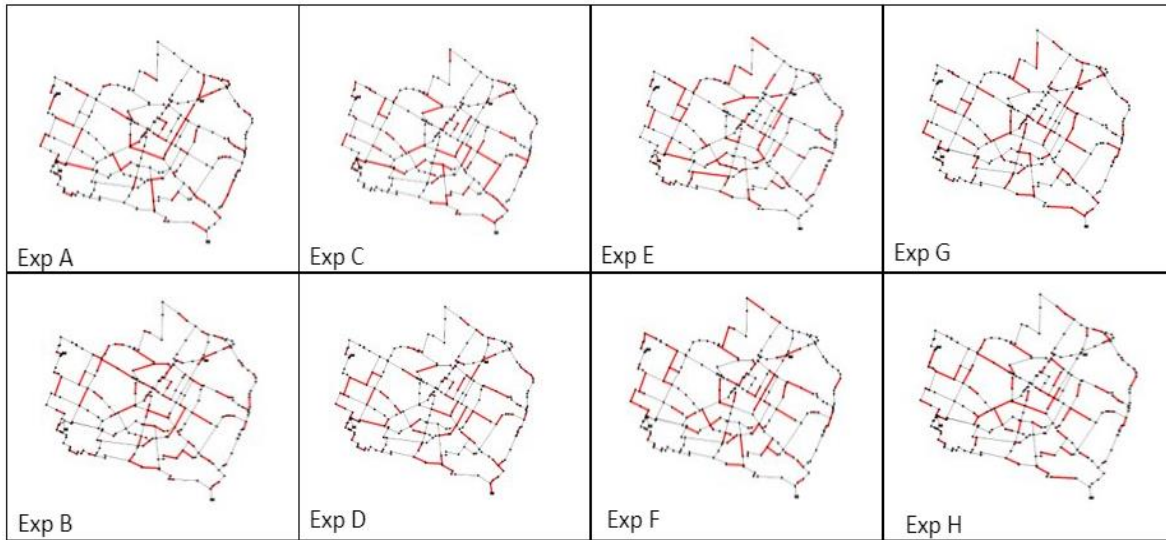


Figure 4.9: Critical pipes identified for different experiments (Budget \$10 million)

4.3. DISCUSSION

A methodology was developed to integrate the uncertainties of network hydraulic parameters with a proactive seismic rehabilitation decision-making model and identify the critical pipes of the network for a limited budget-constraint. Three network hydraulic parameters were selected, and a full-factorial design of experiment was developed to identify the individual and combined effect of the selected parameters. The analysis was conducted for four budget constraints. The maximum value of expected PSSI was impacted due to the integration of uncertainties of network hydraulic parameters. The value of PSSI depends on the hydraulic simulation of the network and the uncertainty associated with hydraulic network parameters impact the seismic rehabilitation decision and identified critical pipes for same budget constraint.

CHAPTER 5 : EFFECTS OF DEGRADATION ON SEISMIC REHABILITATION DECISION-MAKING FOR WATER PIPE NETWORKS

Proactive seismic rehabilitation decision-making methods are necessary to ensure maximum serviceability after a seismic event. Most recent proactive seismic rehabilitation decision-making models of water distribution networks are sensitive to network hydraulics and pipe fragilities. Although network hydraulics and pipe fragilities are influenced by the pipe degradations, the effects of degradation on proactive seismic rehabilitation decision-making were not studied. The probabilistic nature of the water pipe degradation makes the consideration of degradation challenging. This research aims to investigate the effects of the degradation of pipes on the seismic rehabilitation decision-making of water distribution networks. The methodology includes (1) designing simulation experiments; (2) integrating the effects of inside and outside degradation with seismic rehabilitation decision-making; (3) conducting statistical analysis to identify the effects of integrating the pipe degradation. The simulation experiments were designed to investigate the effects of degradation on the inside surface of pipes and on the outside surface of pipes individually and combinedly. Fragility curves were modified to consider degradation based on the probabilistic stress change of pipe with age. The probabilistic nature of the pipes' outside degradation rate was considered to determine the probabilistic value of stress change. A probabilistic pipe roughness growth rate model was used to modify the hydraulic modeling of pipe considering pipes' inside degradation. Modified seismic fragility curves and the modified value of the Hazen-Williams roughness coefficient were integrated to consider the effects of degradation based on the designed simulation experiment. A simulated annealing-based optimization approach was used to identify the critical pipes and associated maximum serviceability for each experiment and each budget constraint. The Analysis of Variance (ANOVA) test and Tukey statistical tests were conducted to identify the statistical significance of the effect of integrating degradation. The application of the proposed approach was illustrated on a benchmark network. Five rehabilitation budget constraints were selected for this study. Critical pipes were identified for each rehabilitation budget constraint based on the optimization algorithm. The results for each simulation experiment showed that the identified critical pipes were different. The associated maximum serviceability was reduced for the same budget constraints if outside and inside degradation was considered individually and

combinedly. The changes in identified critical pipes and associated maximum serviceability due to the consideration of outside and inside degradation implies the dependency of proactive seismic rehabilitation decision-making model on outside and inside degradation. The statistical test results imply that the degradation of pipes of the water distribution network has an impact on seismic rehabilitation decision-making models of water distribution networks. Therefore, it is recommended to integrate the degradation effect with existing seismic rehabilitation decision-making models.

5.1. METHODOLOGY

To investigate the effects of the pipes' outside and inside degradation on the seismic rehabilitation decision-making for water distribution networks, this study was divided into three steps: (1) designing simulation experiments; (2) integrating the effects of inside and outside degradations with seismic rehabilitation decision-making; (3) conducting statistical analysis to identify the impacts of integrating the pipe degradation. Each step is discussed in the subsequent section of the paper.

5.1.1. Design of Simulation Experiment

The effects of degradation of pipes of a water distribution network can be classified into two groups: reduction of thickness due to corrosion at the outer surface of pipes (Ji et al. 2017, Mazumder et al. 2020a; Mazumder et al. 2020b) and change in the roughness of pipes due to deposition inside the pipes (Seifollahi- Aghmiuni et al. 2013; Abdel-Monim et al. 2005).

To investigate the combined and individual effects of these two classified groups of degradation, simulation experiments were designed. Each of the two above-mentioned degradation types (outside surface of pipes and inside surface of pipes) was studied at two levels. Therefore, a 2^2 full factorial design was selected for this study. The levels were coded as +1 (including the effect of that type of degradation) and -1 (excluding the effect of that type of degradation). Table 5.1 presents the selected degradation type with their levels (including effects and excluding effects). The coded design for all simulation experiments is provided in Table 5.2.

Table 5.1: Types of degradation in pipes with their levels of experiment

Types of Degradation	Notation	Level
----------------------	----------	-------

		Including Effect	Excluding Effect
Degradation on Outside Surface of Pipes	A	+1	-1
Degradation on Inside Surface of Pipe	B	+1	-1

Table 5.2:Simulation experiment design matrix

Experiment Name	Experiment Notation	A	B
Experiment 1	Exp_001	-1	-1
Experiment 2	Exp_002	+1	-1
Experiment 3	Exp_003	-1	+1
Experiment 4	Exp_004	+1	+1

5.1.2. INTEGRATION OF EFFECT OF DEGRADATION ON OUTSIDE SURFACE OF PIPE

The reduction of thickness due to corrosion on the pipes can be classified as general corrosion, patch corrosion, and pitting corrosion (Rajeev et al. 2014). Pitting corrosion is considered more dangerous than uniform corrosion because it generates more stress in the pipeline (Mazumder et al. 2020b). In this study, pitting corrosion was considered to investigate the effects of thickness loss on the outer surface of the pipes.

In existing seismic rehabilitation decision-making models, the pipe damage rate after earthquakes is represented by the repair rate, defined as the number of repairs per pipe unit length. To investigate the influence of degradation on the seismic performance of water distribution networks, a modified ALA equation was used to calculate the seismic repair rate (Mazumder et al. 2020b). The repair rate was calculated using Eq. (5.1).

$$\text{Seismic Repair Rate, } SRR = K_p * K1 * 0.00187 * PGV \quad (5.1)$$

where, K_p is the physical modification factor calculated based on time variant stress on pipeline, $K1$ is the modification factor that was obtained from ALA.

K_p was defined as the ratio of the corroded pipe's stress to the uncorroded pipe's stress. The value K_p was calculated using Eq. (5.2) (Mazumder et al. 2020b).

$$K_p = \frac{\sigma_T}{\sigma_{T_0}} \quad (5.2)$$

where,

σ_T = Stress at the time T due to pitting corrosion at outside surface of pipes

σ_{T_0} = Stress on the pipeline at the time of installation

The value of σ_{T_0} was calculated using Eq. (5.3) (Robert et al. 2016)

$$\frac{\sigma_{T_0} * D^2}{W + \gamma * D^2 * h} = \alpha_1 * \left(\frac{E_p}{E_s}\right)^{\beta_1} \left(\frac{E_s}{\gamma * h}\right)^{\beta_2} * \left(\alpha_2 \frac{\left(\frac{P}{E_s}\right)^{\beta_3}}{\left(\frac{d}{D}\right)^{\beta_4} \left(\frac{W}{\gamma * D^2 * h} + 1\right)^{\beta_5}} + \alpha_3 \frac{\left(\frac{d}{D}\right)^{\beta_6} * \left(\frac{W}{\gamma * D^2 * h} + 1\right)^{\beta_7}}{\alpha_4 \left(\frac{E_p}{E_s}\right)^{\alpha_4} + \alpha_5 \left(\frac{P}{E_s}\right)^{\alpha_5} + \alpha_6 \left(\frac{h}{D}\right)^{\alpha_6} + \alpha_7 \epsilon}\right) \quad (5.3)$$

where, ϵ is the model uncertainty coefficient; W is the traffic load (kN); γ is the unit weight of soil (kN/m³); D is the nominal diameter of the pipeline after time T (mm); h is the buried depth of pipeline (m); P_0 is the water pressure of the pipeline (kPa); d is the pipes' wall thickness (mm); E_p is the elastic modulus of pipe material (MPa), E_s is the elastic modulus of soil (MPa), Model coefficients, α and β , can be taken from Robert et al. (2016) (α_1 : 0.12, α_2 : 4.08, α_3 : 1.76E+06, α_4 : 7.65E+04, α_5 : 4.17E+06, α_6 : -3.23E+07, α_7 : -3.55E+07, β_1 : 0.086, β_2 : 0.94, β_3 : 0.89, β_4 : 0.88, β_5 : 0.94, β_6 : -0.51, β_7 : -0.71).

Stress on a pipeline after time T was calculated by substituting d_e in place of d in Eq. (3), where d_e is the effective remaining wall thickness after time T. The value of effective thickness was calculated using Eq. (5.4) (Ji et al. 2017).

$$d_e = d - \tau(T) \quad (5.4)$$

where $\tau(T)$ is the corroded depth when the pipe age is T years. The value of $\tau(T)$ is probabilistic in nature and follows generalized extreme value (GEV) distribution. Eq. (5.5) was used to predict the value of $\tau(T)$ (Wang et al. 2019).

$$\tau(T) = (\rho n + \sqrt{1 - \rho^2 n^*}) T^n \quad (5.5)$$

where, $[n, n^*: GEV(\mu_G, \sigma_G, \epsilon)]$;

$\rho = -0.55$; $\mu_G = 0.6204$; $\sigma_G = 0.2919$; $\epsilon = -0.2816$.

Pipe stress varies due to uncertainties of pipe geometries, pipe material, and external loads. To consider the stress variation, probability-based analysis was performed in the present study. Six

parameters (bury depth, soil elastic modulus, soil unit weight, traffic load, pipe’s wall thickness, and model uncertainty) were selected as random variables. The mean value, coefficient of variance, and distribution type for the six variables are presented in Table 5.3.

Table 5.3: Typical statistical information of physical properties in pipeline analysis

Physical Parameter		Mean	Coefficient of Variation (CV)	Distribution	Reference
Location	Bury depth, h	0.8 m	0.25	Normal	Ji et al. 2017; International Plumbing Code 2015
Backfill Soil	Elastic Modulus, E_s	25 MPa	0.3	Lognormal	Empirical Value
	Unit Weight, γ	20 kN/m ³	0.1	Lognormal	Empirical Value
Load	Traffic Load, W	50 kN	0.3	Normal	Ji et al. 2017
Model Uncertainty	ϵ	1	0.15	Normal	Ji et al. 2017
Pipe Properties	Wall thickness, d	12-20 mm		Beta	Ji et al. 2017

5.1.3. Integration of Effect of Degradation on Inside Surface of Pipes

The Hazen-Williams equation was used in this study for hydraulic analysis. The Hazen-Williams equation to calculate the flow velocity is as follows:

$$v = k \cdot C \cdot R^{0.63} \cdot S^{0.54} \quad (5.6)$$

where, k is the conversion factor, C is the roughness coefficient, R is the hydraulic radius in ft or m, S is the slope of the energy line, and v is the velocity of water in ft/s or m/s.

Water pipes tend to accumulate corrosion byproducts and suspended particles. The roughness of a pipe changes due to the accumulation of corrosion byproducts. The value of C reduces with respect to time because of degradation (Seifollahi-Aghmiuni et al. 2013; Jacimovic et al. 2015). The value of C was determined in different time steps for modeling the effects of degradation. Eq. (5.7) was used to calculate the value of the value of C after a certain age (Sharp and Walski 1988).

$$C_p^T = 18 - 37.2 * \log \left(\frac{e_{0p}^T + T * a_p^T}{D_p} \right) \quad (5.7)$$

Where, C_p^T is the Hazen-Williams coefficient in pipe p at year T, e_{0p}^T is the initial roughness of the pipe; a_p^T is the roughness growth rate of the pipe, D_p is the diameter of pipe p (mm). The value of e_{0p}^T and a_p^T was calculated using Eq. (5.8) and Eq. (5.9).

$$\log \left(e_{0p}^T \right) = \frac{C_p^{T-1} - 18}{-37.2} + \log(D_p) \quad (5.8)$$

$$a_p^T = \frac{10^{\frac{0.5 * C_p^{T-1} - 18}{-37.2}} * D_p - e_{0p}^T}{50} \quad (5.9)$$

In Eq. (5.8) and Eq. (5.9), C_p^{T-1} was considered equal to the value C which is obtained from network properties at time T=0.

To consider the associated uncertainties, the value of the C was considered normally distributed for this study with a coefficient of variation (CV) value equal to 0.2 (Roy et al. 2021). The procedure of calculating the probabilistic value of Hazen-Williams roughness coefficient for pipe p after year T (C_p^T) is described in Figure 5.1.

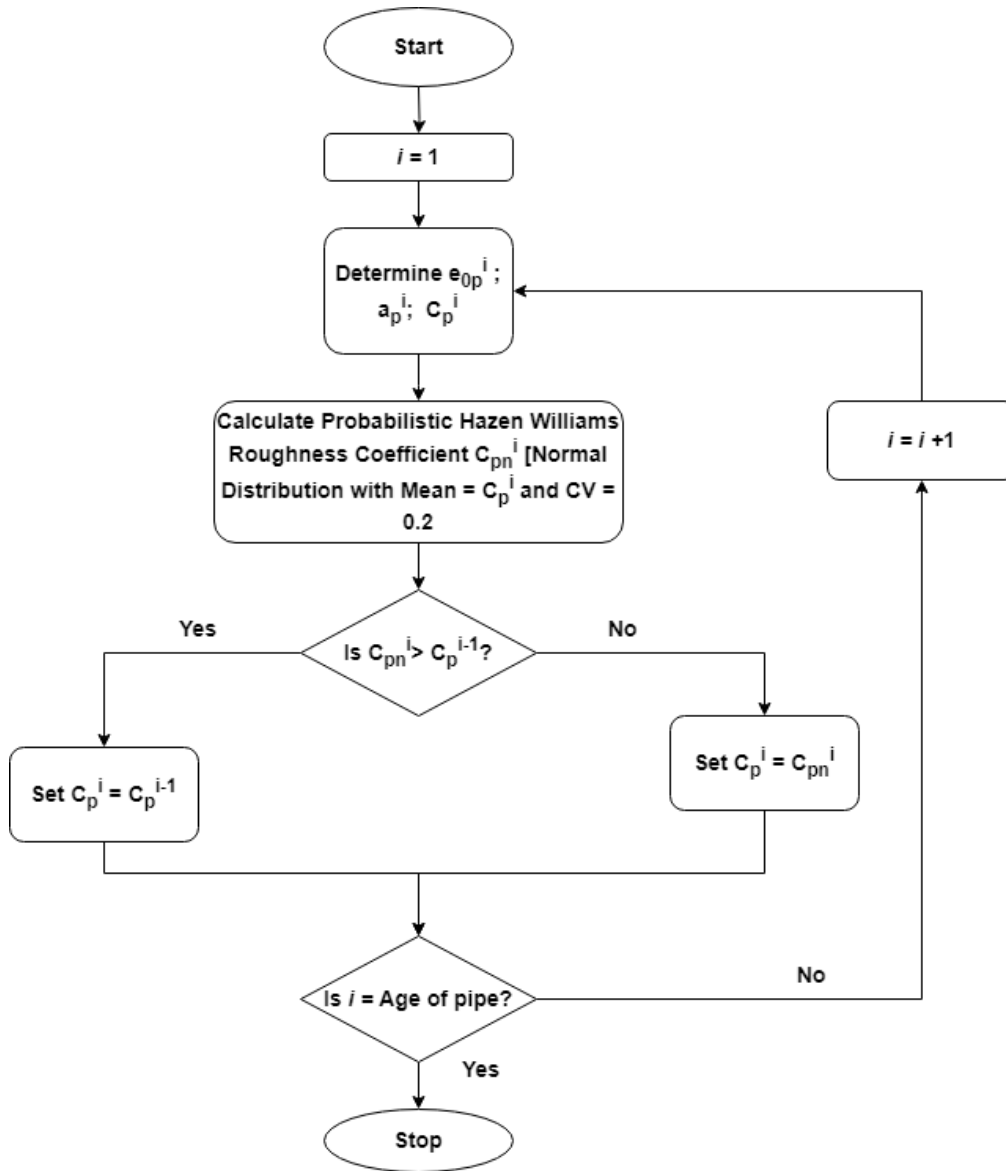


Figure 5.1: Steps of calculating the probabilistic value of Hazen-Williams roughness coefficient for pipe p after year T (C_p^T)

5.1.4. Seismic Rehabilitation Decision-Making

The objective was to maximize the serviceability of a water distribution network after an earthquake event for a specific budget limit and propose an optimal rehabilitation policy to achieve that serviceability. Post-earthquake Serviceability Index (PSSI) was used as a post-earthquake serviceability indicator (Roy et al. 2022; Wang et al. 2010).

The objective function for the optimization problem was developed as follows:

$$\max_{\mathbf{x} \in \mathbf{X}} E [PSSI(\mathbf{x})] \quad (5.10)$$

subject to

$$C(x) \leq Cmax$$

where, X is the set of all rehabilitation policies, $C(x)$ is the total cost to rehabilitate based on policy x , $Cmax$ is the maximum available budget for rehabilitation. $E[PSSI(x)]$ is the average value of PSSI for all Monte Carlo runs and all random peak ground velocity fields. The equation for calculating the value of $E[PSSI(x)]$ is as follows (Shahandashti and Pudasaini 2019):

$$E[PSSI(x)] = \frac{\sum_{i=1}^k \sum_{m=1}^M PSSI}{k \cdot M} \quad (5.11)$$

where, k is the total number of random peak ground velocity fields and M is the maximum number of Monte Carlo runs. The maximum number of Monte Carlo runs was selected based on a convergence study (Shahandashti and Pudasaini 2019).

The average value of PSSI for each random peak ground velocity field was calculated based on Eq. (5.12).

$$Average PSSI = \frac{(\sum_{m=1}^M PSSI)}{M} \quad (5.12)$$

The steps for calculating the value of $E[PSSI(x)]$ for each rehabilitation policy and the average PSSI for each peak ground velocity field are demonstrated in Figure 5.2 (Shahandashti and Pudasaini 2019).

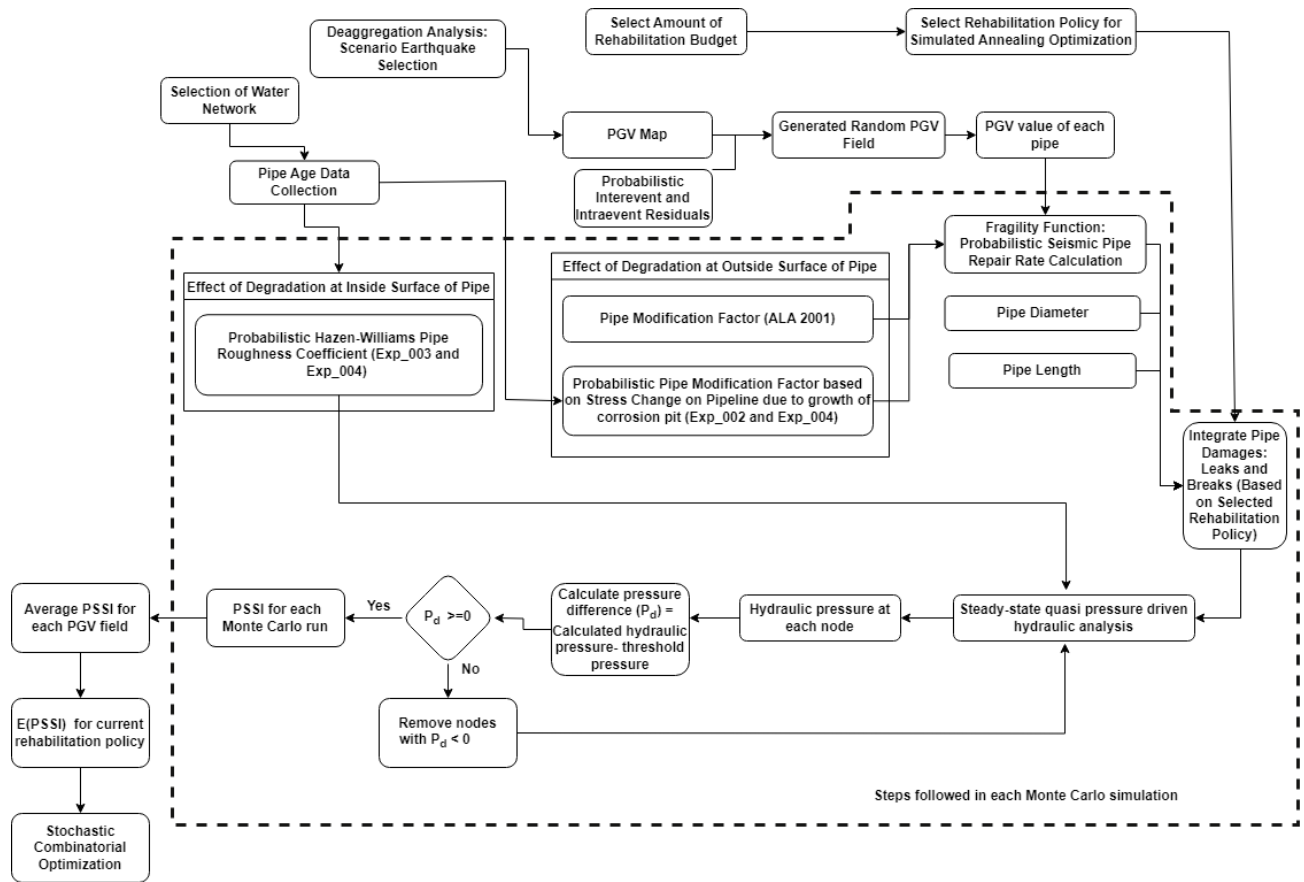


Figure 5.2: Steps of determining the value of $E[PSSI(x)]$ for each rehabilitation policy and average PSSI for each PGV field

The effects of degradation on the inside surface of the pipes and the outside surface of pipes were integrated according to the design of experiment. The same methodology described in section 3.1.3 and 3.1.4 was used to calculate the seismic repair rate of each pipe. Using a simulated-annealing (SA) -based optimization algorithm, the critical pipes were identified, and the maximum value of $E[PSSI(x)]$ was calculated for each experiment and for the maximum rehabilitation budget available (Shahandashti and Pudasaini 2019). The values of average PSSI for each random peak ground velocity field of the optimized rehabilitation policy were stored for statistical analysis.

5.1.5. Statistical Analysis to Investigate the Effect of Degradation

Two statistical tests were conducted to investigate both combined and individual effects of two types of degradation on seismic rehabilitation decision-making models of water pipe networks. The ANOVA test and the Tukey test were used in this study. For each simulation experiment, the

ANOVA test can determine the difference among the average PSSI. The null hypothesis mentioned in Eq. (5.13) was tested in the ANOVA test:

$$H_0 = \mu_1 = \mu_2 = \dots = \mu_k \quad (5.13)$$

where μ is the maximum $E[\text{PSSI}]$ value for each experiment; and k is the number of experiments. If the ANOVA test result is not significant (i.e., p value is less than the level of significance), the null hypothesis is accepted, implying that the change in the values of average PSSI due to the consideration of impacts of outside and inside degradation is not statistically significant. If the ANOVA test result is significant, the null hypothesis is rejected. The rejection of the null hypothesis implies that there are at least two different individual simulation experiments.

The Tukey test was conducted to identify which simulation experiments differed as the ANOVA test could not identify which specific simulation experiments were different.

5.2. APPLICATION AND RESULTS

5.2.1. Selection of Network

Modena network (Figure 5.3) was used to illustrate the approach described in this study (Center of Water Systems 2018). The properties of the Modena network are tabulated in Table 5.4.

Table 5.4: Properties of Modena network

Junction	268
Pipes	317
Reservoirs	4
Total Length of Pipe	71,806.11m

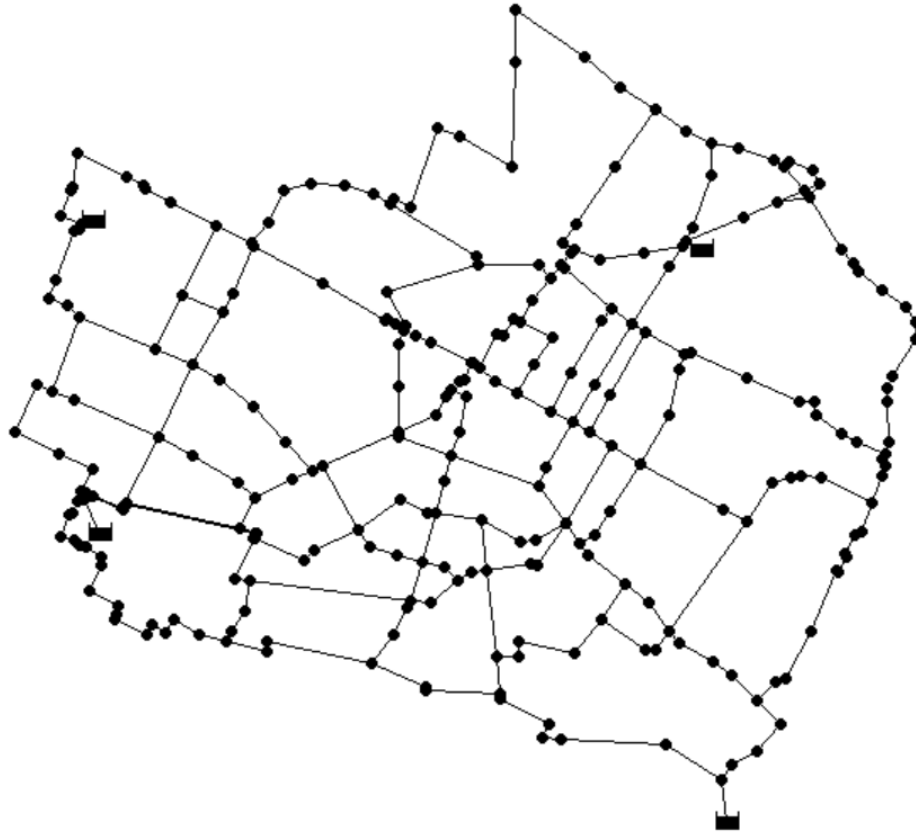


Figure 5.3: Layout of Modena network

5.2.2. Assumptions for this study

Pipe Materials and Joints of Modena Network

For the properties of pipe materials, pipes were assumed to consist of two types: cast-iron (diameter less than 300 mm or 12 inches) pipes with lead joints and ductile-iron pipes (diameter more than 300 mm or 12 inches) with rubber gasketed joints.

Age of Pipes of Modena Network

As the Modena network is a benchmark network for study purposes only, the age of the network pipes was not available. For this study, the age of each pipe was assumed randomly between 30 years to 70 years. The age of the pipes of the Modena network is demonstrated in Figure 5.4.

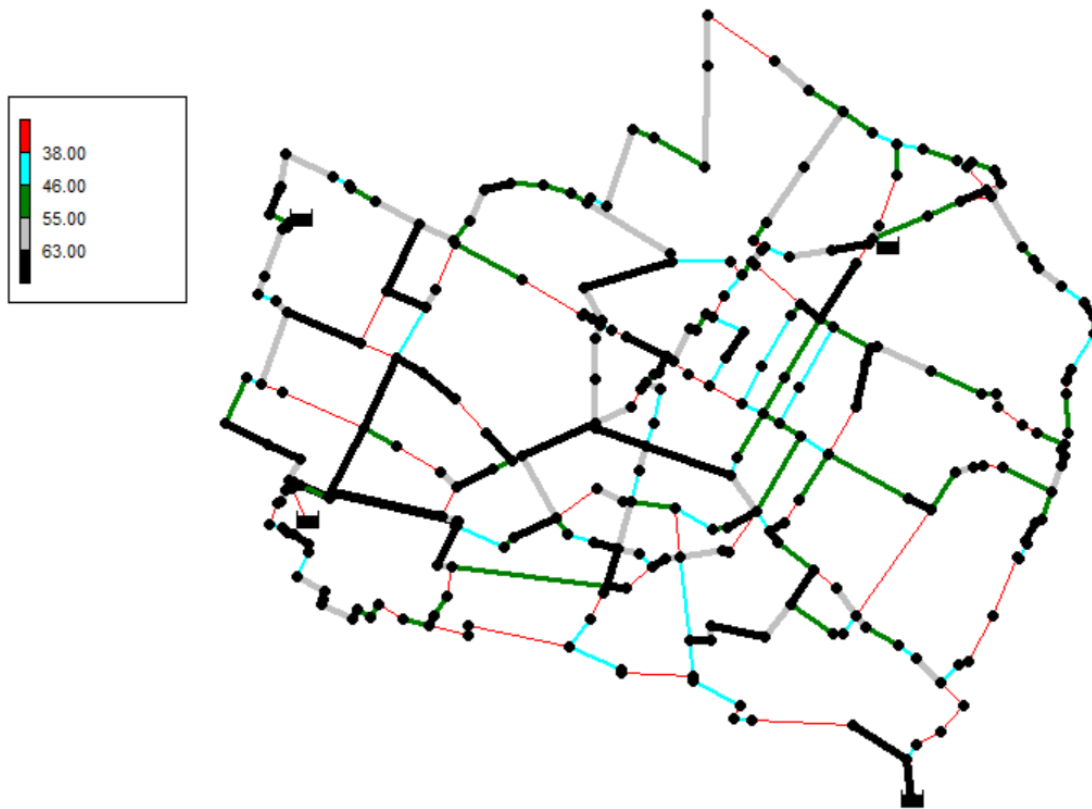


Figure 5.4: Layout of Modena network with ages (in year) of different pipes

5.2.3. Cost Boundaries

The study was conducted for five cost boundaries: \$2.5 million, \$5 million, \$7.5 million, \$10 million, and \$12.5 million. Following the previously described approach, the critical pipes were replaced with earthquake-resistant ductile iron (DI) pipes as these pipes have no record of any leaks and breaks in some major earthquakes in Japan in which almost all other utilities and infrastructures were severely affected (Haddaway 2015). Therefore, for this study, the critical pipes were assumed to be replaced with earthquake resistant pipes during seismic rehabilitation of the pipe network. The cost data used for the rehabilitation are summarized in Table 4.3.

5.2.4. Deaggregation Analysis and Calculation of PGV

For the deaggregation analysis, we assumed that the centroid of the network was in California (city of Pasadena). Deaggregation analysis was conducted at the location of the network (34.146267° N, 118.144040° W) to identify the scenario earthquake (Shahandashti and Pudasaini 2019).

For the selected scenario earthquake, the value of PGV (Peak Ground Velocity) for each pipe was calculated (Shahandashti and Pudasaini 2019; USGS 2018a; USGS 2018b). For this study, 20 random PGV fields were generated by integrating probabilistic inter-event and intra-event residuals ($k=20$). The peak ground velocity (PGV) for each pipe was determined for each random peak ground velocity field.

Post-earthquake system serviceability index (PSSI) is used as a serviceability measure for this study (Wang 2010; Shi 2006). The same methodology described in section 3.1.3 and 3.1.4 was used to calculate the seismic repair rate of each pipe. After calculating the repair rate of each pipe, PSSI was calculated for each random PGV (Shahandashti and Pudasaini 2019). The generated peak ground velocity field is shown in Figure 4.3. Figure 4.4 shows the same peak ground velocity field magnified to the scale of the network for Modena network.

5.2.5. Selection of the maximum number of Monte Carlo runs:

A convergence study was conducted to identify the maximum number of Monte Carlo runs considering pipe degradation. The results of the convergence study are shown in Figure 5.5.

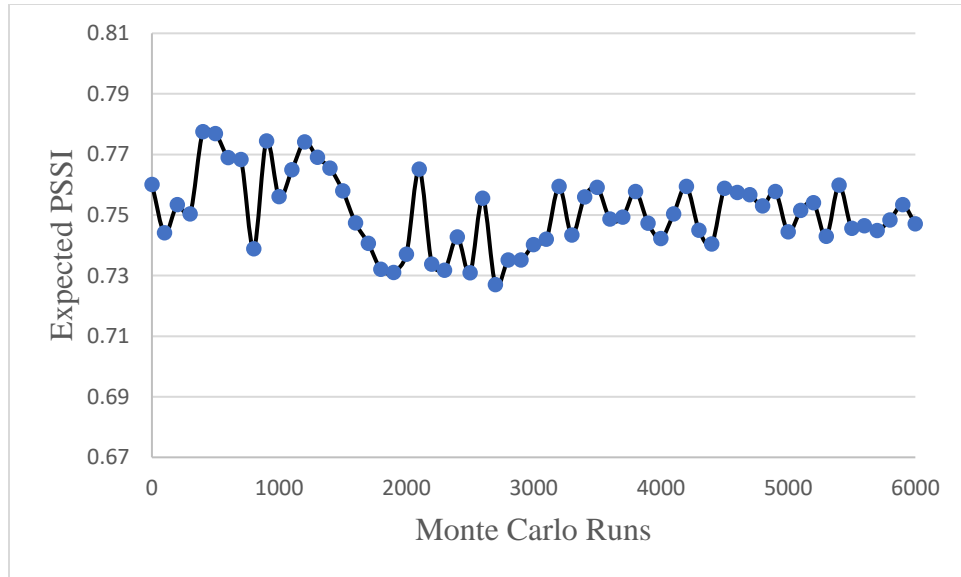


Figure 5.5: Summary of convergence study result

According to the convergence study, approximately 3000 Monte Carlo runs were sufficient for the analysis ($M = 3000$).

5.2.6. Results: Identification of Critical Pipes

Using the described approach for each cost boundaries, critical pipes were identified for each experiment for the Modena network. Figure 5.6 shows the value of maximum E[PSSI] for each experiment and each cost boundary.

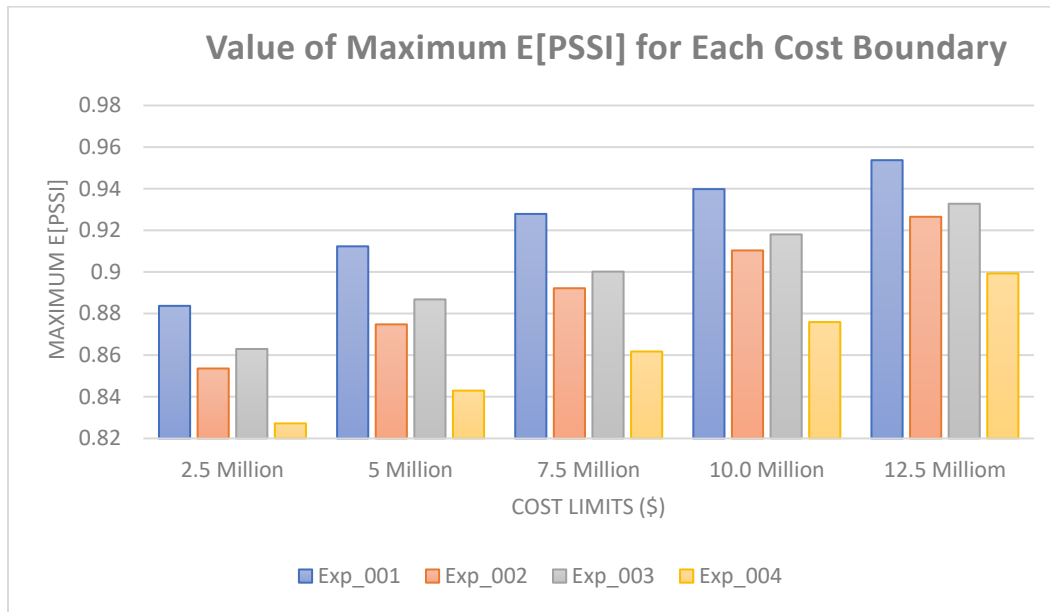


Figure 5.6: Value of maximum E[PSSI] for each cost boundary

The maximum value of E[PSSI] is changing due to the consideration of pipes' inside and outside degradation. For the same budget limitation, the value of maximum E[PSSI] is reduced by 3-4% due to pipes' outside degradation. The value of E[PSSI] is getting reduced by 2-3% due to pipes' inside degradation. The value of E[PSSI] is getting reduced by 6-7% due to the consideration of pipe's inside and outside degradation combinedly.

The critical pipes identified for each experiment are shown in Figure 5.7 using highlighted lines for rehabilitation budget of 2.5 million. The critical pipes are highlighted with black color.

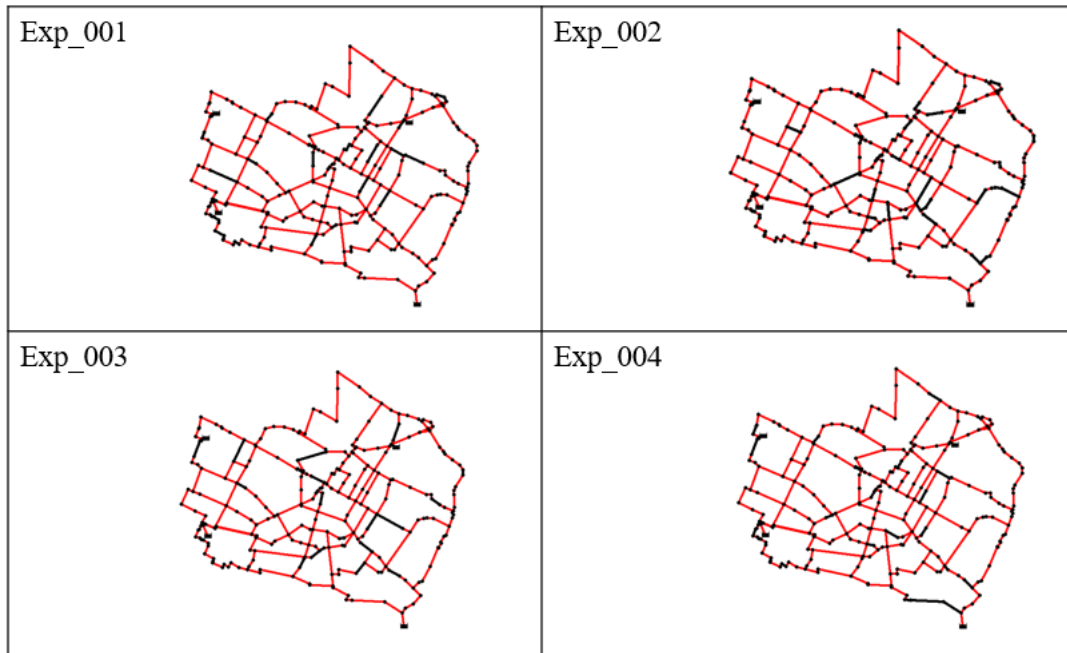


Figure 5.7: Identified critical pipes for different experiments using a cost boundary of 2.5 million. Similarly, the critical pipes identified for each experiment are shown in Figure 5.8 using highlighted lines for rehabilitation budget of 5 million.

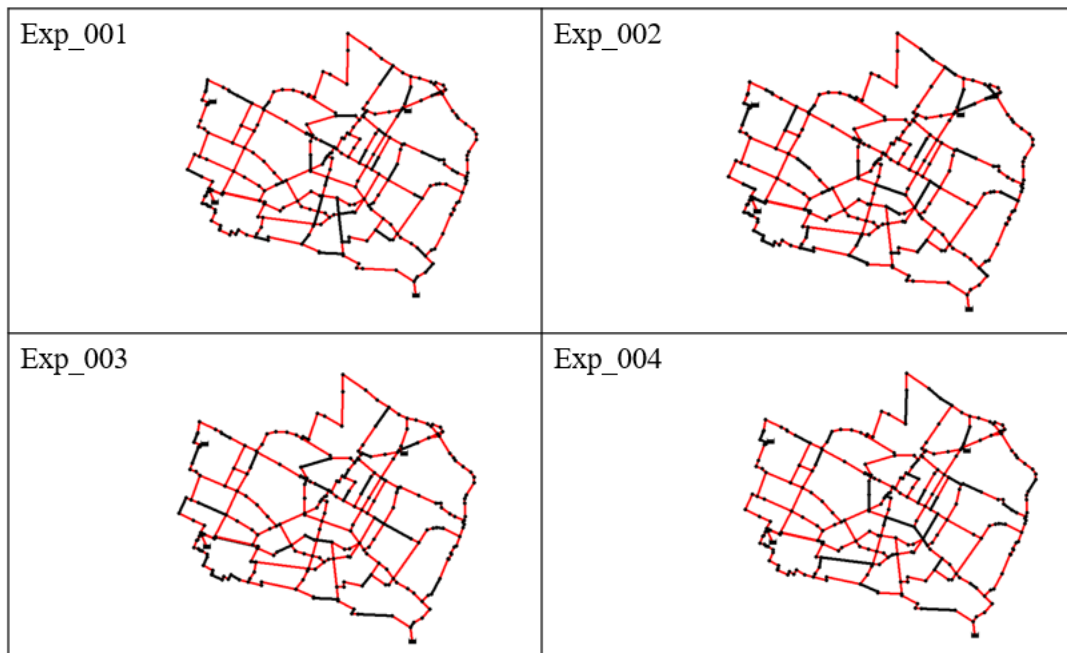


Figure 5.8: Identified critical pipes for different experiments using a cost boundary of 5 million.

The critical pipes identified for each experiment are shown in Figure 5.9 using highlighted lines for rehabilitation budget of 7.5 million.

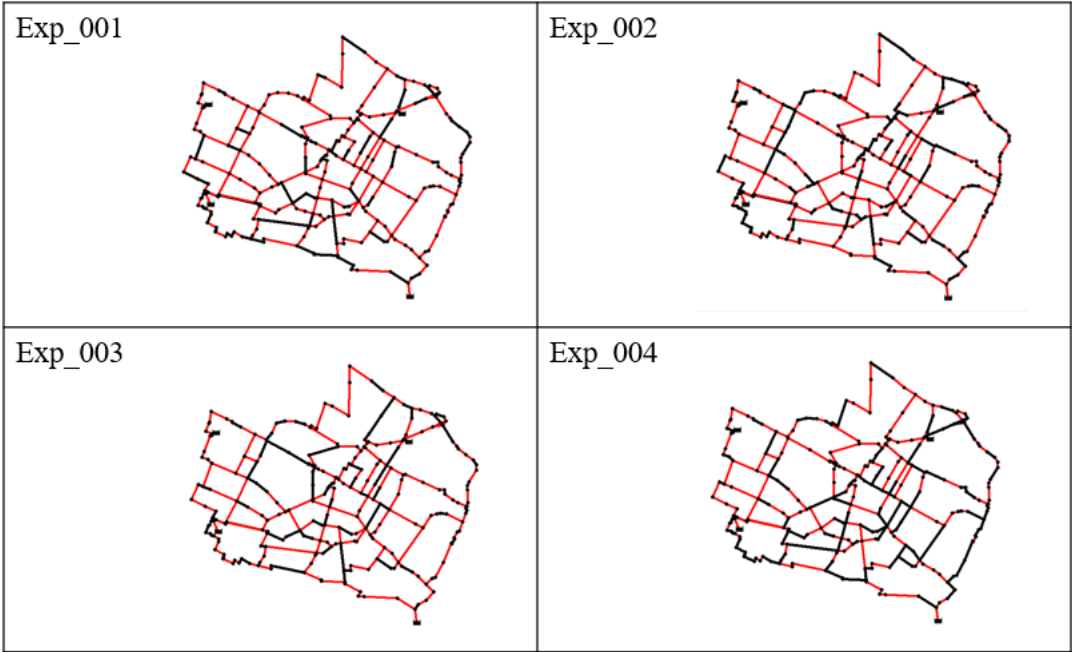


Figure 5.9: Identified critical pipes for different experiments using a cost boundary of 7.5 million

The critical pipes identified for each experiment are shown in Figure 5.10 using highlighted lines for rehabilitation budget of 10 million.

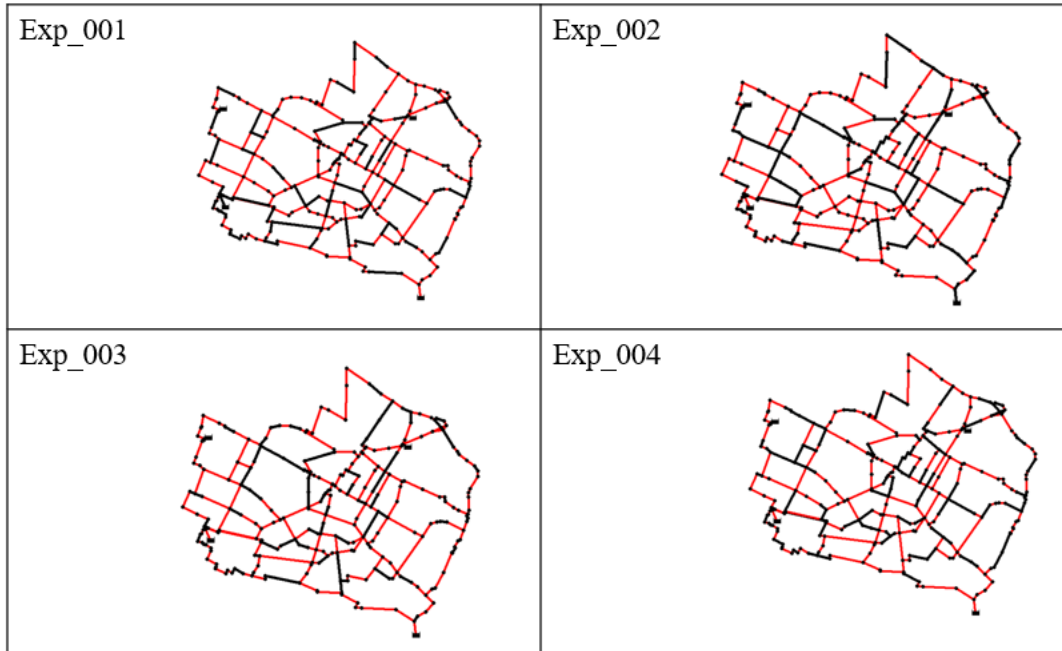


Figure 5.10: Identified critical pipes for different experiments using a cost boundary of 10 million

The critical pipes identified for each experiment are shown in Figure 5.11 using highlighted lines for rehabilitation budget of 12.5 million.

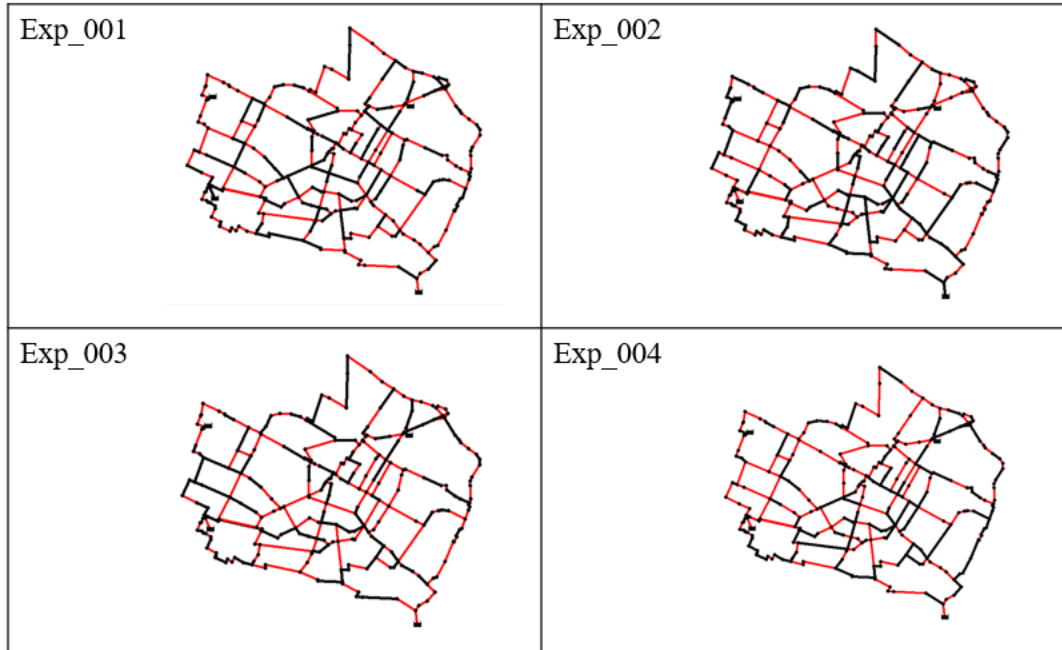


Figure 5.11: Identified critical pipes for different experiments using a cost boundary of 12.5 million

Identified critical pipes shown in Figure 5.7 to Figure 5.11 indicate the effect of degradation on seismic rehabilitation decision-making. Figure 5.7 to Figure 5.11 demonstrate that the consideration of the effects of outside degradation and inside degradation of pipes both individually and combinedly has an impact on selection of critical pipes.

Table 5.5 summarizes the total simulation hours to solve the optimization problem using simulated annealing-based optimization algorithm along with the actual cost to adopt the optimized rehabilitation policy for each experiment and for each cost boundary.

Table 5.5: Summary of solution of simulated annealing optimization

Cost Boundary (Million)	Exp_001		Exp_002		Exp_003		Exp_004	
	Simulation Hours (h) ^a	Actual Cost (USD)	Simulation Hours (h) ^a	Actual Cost (USD)	Simulation Hours (h) ^a	Actual Cost (USD)	Simulation Hours (h) ^a	Actual Cost
2.5	298.47	2,499,895.84	295.53	2,499,940.86	293.37	2,499,450.11	292.61	2,499,244.81
5.0	296.12	4,999,732.47	297.82	4,990,751.39	290.97	4,999,680.29	295.09	4,999,637.22
7.5	288.96	7,4999,917.51	292.31	7,499,881.68	289.29	7,493,899.13	288.62	7,4959,397.51
10.0	284.51	9,999,312.92	283.58	9,999,476.44	288.42	9,999,360.33	289.88	9,999,841.92

12.5	291.81	12,499,431.09	289.62	12,490,762.99	291.53	12,499,422.62	285.51	12,499,169.09
------	--------	---------------	--------	---------------	--------	---------------	--------	---------------

^a Solution time using AMD Ryzen 5 5500U with Radeon Graphics 2.10 GHz Processor with 16.0 GB Ram and 64-bit operating system

5.2.7. Results: Statistical Analysis

To identify the statistical significance of integrating water pipe degradation, the null hypothesis (H_0) and the alternative hypothesis (H_1) were identified.

Null hypothesis, $H_0: \mu_1 = \mu_2 = \dots = \mu_4$

Alternative hypothesis, $H_1: \mu_1 \neq \mu_2 \neq \dots \neq \mu_4$

Level of Significance: 5%

The one-way ANOVA test result shows that the value p was 0.0257, 0.0324, 0.0231, 0.0219, and 0.0268 for cost boundaries 2.5 million, 5 million, 7.5 million, 10 million, and 12.5 million respectively, which are less than 0.05 (5% level of significance). Therefore, there were statistically significant differences between the values of average E[PSSI] for at least two different simulation experiments. The Tukey test (multiple pairwise comparisons test) was conducted to identify the simulation experiments that have statistically significant differences. As this study was conducted to determine the effects of degradation, three pairs were used for the Tukey test, comparing the no-degradation experiment (Exp_001) with the other experiments: (Exp_001, Exp_002); (Exp_001, Exp_003); (Exp_001, Exp_004). Table 6 summarizes the results of the Tukey test.

Table 5.6: Summary of Tukey test result

Cost Boundary	Group 1	Group 2	meandiff	p -adj	Reject
\$2.5 million	Exp_001	Exp_002	0.0301	0.0013	TRUE
	Exp_001	Exp_003	0.0207	0.0014	TRUE
	Exp_001	Exp_004	0.0565	0.0010	TRUE
\$5 million	Exp_001	Exp_002	0.0375	0.0012	TRUE
	Exp_001	Exp_003	0.0255	0.0012	TRUE
	Exp_001	Exp_004	0.0693	0.0009	TRUE
\$7.5 million	Exp_001	Exp_002	0.0357	0.0014	TRUE
	Exp_001	Exp_003	0.0277	0.0012	TRUE

	Exp_001	Exp_004	0.0218	0.0009	TRUE
\$10 million	Exp_001	Exp_002	0.0294	0.0013	TRUE
	Exp_001	Exp_003	0.0218	0.0013	TRUE
	Exp_001	Exp_004	0.0639	0.0010	TRUE
12.5 million	Exp_001	Exp_002	0.0272	0.0013	TRUE
	Exp_001	Exp_003	0.0209	0.0012	TRUE
	Exp_001	Exp_004	0.0544	0.0010	TRUE

The Tukey test results for the Modena network show that the null hypothesis was rejected for all three pairwise comparisons, and it was concluded that the effects of the pipe degradation were significant.

It was be concluded from the ANOVA test and Tukey test results that the effect of degradation on the outside surface of pipes (Exp_002) and the inside surface of pipes (Exp_003) has a statistically significant impact on the proactive seismic rehabilitation decision-making models. The combined effect (Exp_004) of degradation on outside surface of pipes and inside surface of pipes also statistically significant on proactive seismic rehabilitation decision-making models.

5.3. DISCUSSION

Existing seismic rehabilitation decision-making models depends on the hydraulic properties of water pipe network to identify the performance of the network after the seismic event and physical properties of the network to identify the probabilistic location of the damages after an earthquake event. Degradation of pipes of a water pipe network can affect both hydraulic properties and physical properties of a water pipe network. A methodology has been proposed to identify the effects degradation on seismic rehabilitation decision-making of water pipe networks. A simulation experiment has been developed to investigate the effects of degradation on the outside surface and inside surface of pipes individually and combinedly. A method was developed to integrate the probabilistic nature of water pipe degradation.

The maximum value of expected PSSI and the identified critical pipes for same amount of budget constraint were impacted due to the integration of degradation. The value of repair rate and the value of PSSI depends on the physical properties and hydraulic properties of the network

respectively. The probabilistic nature of degradation is impacting the hydraulic properties and physical properties of the network and impacting the decision-making.

To identify the statistical significance of this difference, two statistical tests were conducted for all budget constraints. The statistical analysis results show that the effect degradation is statistically significant for all budget constraints considering a 5% level of significance.

CHAPTER 6 : CONCLUSION

6.1. SUMMARY OF RESULTS

In chapter 3, a methodology has been proposed to identify the effects of water pipe network uncertainties on seismic vulnerability assessment of networks. Three water pipe network uncertainties were selected: uncertainties in nodal demand, reservoir head, pipe roughness coefficient. Two different networks were used to apply the proposed methodology.

The statistical analysis results show that the individual effect of uncertainty of demand and uncertainty of pipe roughness coefficient can be ignored for the fixed value of coefficient of variation ($CoV = 0.2$). On the contrary, the individual effect of uncertainty of reservoir head is statistically significant for the selected value of CoV ($CoV = 0.2$). The combined effect of uncertainty of the selected water pipe network uncertainties is statistically significant.

Based on the results from sensitivity analysis, the individual effect of uncertainty of reservoir head is found to be statically significant, even at low levels of uncertainty (minimum value of $CoV = 0.01$). By contrast, the individual effects of demand and pipe roughness coefficient uncertainties are statistically significant for higher levels of uncertainties (CoV ranges from 0.03 to 1).

Based on the results of statistical analysis and sensitivity analysis, it can be concluded that selected water pipe network uncertainties have statistically significant effects on the value of SSI. Therefore, it is highly recommended that water pipe network uncertainties be integrated with seismic vulnerability assessment of water pipe networks.

From the analysis and optimization results of chapter 4, it can be concluded that there is a significant impact of selected network uncertainties on proactive seismic rehabilitation decision-making for the selected values of coefficient of variation. The value of PSSI reduces by 3-4% due to the consideration of all three network uncertainties. The value of PSSI reduces by 1-2% if only one network uncertainty is considered. So, it is recommended to include selected water network uncertainties with the current seismic rehabilitation decision-making model. Future studies are recommended to investigate the impact of other water pipe network uncertainties that were not considered in this study.

From the analysis and results of chapter 5, a methodology has been proposed to identify the effects degradation on seismic rehabilitation decision-making of water pipe networks. A simulation experiment was developed to investigate the effects of degradation on the outside surface and inside surface of pipes individually and combinedly. A method was developed to integrate the probabilistic nature of water pipe degradation. The Modena network was used to apply the proposed methodology. Five different cost boundaries were selected for the study. A simulated-annealing based approach was used to identify the critical pipes for seismic rehabilitation and associated serviceability for each budget constraint.

The optimization results show a difference in the maximum value of serviceability for each budget constraint. The maximum value of serviceability can be reduced by 3-4% for the same budget constraints if the degradation on the outside surface of the pipes is considered. The maximum value of serviceability can be reduced by 2-3% for the same budget constraints if the degradation at the inside surface of the pipes is considered. The maximum value of serviceability can be reduced by 6-7% for the same budget constraints if the degradation on the outside surface and insider surface are considered combinedly.

To identify the statistical significance of this difference, two statistical tests were conducted for all budget constraints. The statistical analysis results show that the effect degradation is statistically significant for all budget constraints considering a 5% level of significance.

Based on the results of simulated annealing and statistical analysis, it can be concluded that degradation of a water pipe network has statistically significant effects on seismic rehabilitation decision-making. Therefore, it is highly recommended that the effects of degradation of water pipe networks should be integrated with existing seismic rehabilitation decision-making models of water pipe networks.

In the analysis and optimization result of chapter 5, a methodology has been proposed to identify the effects degradation on seismic rehabilitation decision-making of water pipe networks. A simulation experiment was developed to investigate the effects of degradation on the outside surface and inside surface of pipes individually and combinedly. A method was developed to integrate the probabilistic nature of water pipe degradation. The Modena network was used to apply the proposed methodology. Five different cost boundaries were selected for the study. A

simulated-annealing based approach was used to identify the critical pipes for seismic rehabilitation and associated serviceability for each budget constraint.

The optimization results show a difference in the maximum value of serviceability for each budget constraint. The maximum value of serviceability can be reduced by 3-4% for the same budget constraints if the degradation on the outside surface of the pipes is considered. The maximum value of serviceability can be reduced by 2-3% for the same budget constraints if the degradation at the inside surface of the pipes is considered. The maximum value of serviceability can be reduced by 6-7% for the same budget constraints if the degradation on the outside surface and insider surface are considered combinedly.

To identify the statistical significance of this difference, two statistical tests were conducted for all budget constraints. The statistical analysis results show that the effect degradation is statistically significant for all budget constraints considering a 5% level of significance.

Based on the results of simulated annealing and statistical analysis, it can be concluded that degradation of a water pipe network has statistically significant effects on seismic rehabilitation decision-making. Therefore, it is highly recommended that the effects of degradation of water pipe networks should be integrated with existing seismic rehabilitation decision-making models of water pipe networks.

6.2. APPLICATION TO INDUSTRY

Water pipe networks must be rehabilitated to improve their resilience against earthquakes and to reduce the direct and indirect losses due to earthquake-induced water main failures. However, one large obstacle to such a task is the huge infrastructure funding gap. This leads to the conclusion that current water pipe networks are highly vulnerable to earthquakes, but the lack of rehabilitation resources renders utilities unable to rehabilitate their entire networks. In such a situation, utilities must identify critical pipes in their networks to maximize the benefit of the limited seismic rehabilitation they can perform. Although many researchers have proposed approaches for seismic vulnerability assessment for the water pipe networks, approaches to identify critical pipes for seismic rehabilitation of a water pipe network are rare. However, even these rare ignored the effects of network uncertainties and pipe degradation. As such, there was a need of an approach to identify critical pipes for proactive seismic rehabilitation of water pipe network that is based on

comprehensive seismic vulnerability assessment; that considers the effect of network uncertainties; pipe degradation; along with the consideration of spatial correlation between seismic intensities; limited rehabilitation budget; and does not ignore the correlation between the effect of pipes' damages on the network serviceability. This model will be beneficial to water utilities of seismic zones to identify the critical pipes of their network considering network uncertainties and pipe degradation for seismic rehabilitation when there is a limited budget available to them.

6.3. FUTURE WORK

This study was conducted to identify the effects of water network uncertainties and effects of degradation of pipe on seismic vulnerability assessment and seismic rehabilitation decision-making of water pipe networks. It is also recommended to consider methods for the investment evaluation under uncertainty, e.g., real option analysis (Zahed et al. 2020; Shahandashti et al. 2023) when evaluating various investment decisions to enhance seismic resiliency of water pipe networks. Role of pipe cost forecasting on proactive seismic rehabilitation decision-making of water pipe networks was not within the scope of this study. Further analysis can be conducted to integrate the role of pipe cost forecasting on proactive seismic rehabilitation decision-making (Kim et al. 2020; Kim et al. 2021a; Kim et al. 2021b). This study was not conducted considering demand surge and life-cycle cost. Further studies can be conducted to identify the role of demand surge (Ahmadi and Shahandashti 2020) and role of life-cycle cost analysis on seismic vulnerability assessment and proactive seismic rehabilitation decision-making of water pipe networks.

REFERENCES

- Abdel-Monim, Y. K., Ead, S. A., & Shabayek, S. A. (2005). Effect of time on pipe roughness. In *17th Canadian Hydrotechnical Conference; Edmonton, Alberta, Canada*.
- Abrahamson, N. A., & Silva, W. J. 2007. "Abrahamson-Silva NGA ground motion relations for the geometric mean horizontal component of peak and spectral ground motion parameters." *Berkeley, CA: Pacific Earthquake Engineering Research Center, Univ. of California*.
- Adachi, T. 2007. *Impact of cascading failures on performance assessment of civil infrastructure systems* (Doctoral dissertation, Georgia Institute of Technology).
- Ahmadi, N., & Shahandashti, M. (2020). Characterizing construction demand surge using spatial panel data models. *Natural Hazards Review*, 21(2), 04020008.
- ALA (American Lifelines Alliance). 2001. *Seismic fragility formulations for water systems*. Washington, DC: ALA.
- Al-Barqawi, H., & Zayed, T. (2006). Assessment model of water main conditions. In *Pipelines 2006: Service to the Owner* (pp. 1-8). [https://doi.org/10.1061/40854\(211\)27](https://doi.org/10.1061/40854(211)27).
- Annus, I., & Vassiljev, A. (2015). Different approaches for calibration of an operational water distribution system containing old pipes. *Procedia Engineering*, 119, 526-534. <https://doi.org/10.1016/j.proeng.2015.08.900>.
- ASCE. (2021). Infrastructure Report Card: Drinking Water.
- Ballantyne, D. B., and Taylor, C. (1990). Earthquake loss estimation modeling of the Seattle water system using a deterministic approach. Kennedy/Jenks/Chilton.
- Bargiela, A., & Hainsworth, G. D. 1989. "Pressure and flow uncertainty in water systems." *Journal of Water Resources Planning and Management*, 115(2), 212-229. [https://doi.org/10.1061/\(ASCE\)0733-9496\(1989\)115:2\(212\)](https://doi.org/10.1061/(ASCE)0733-9496(1989)115:2(212)).
- Barton, N. A., Hallett, S. H., Jude, S. R., & Tran, T. H. (2022). An evolution of statistical pipe failure models for drinking water networks: a targeted review. *Water Supply*, 22(4), 3784-3813. <https://doi.org/10.2166/ws.2022.019>.
- Boskabadi, A., Rosenberger, J. M., & Shahandashti, M. 2020. A Two-Stage Stochastic Programming Approach for Enhancing Seismic Resilience of Water Pipe Networks. In IIE Annual Conference. Proceedings (pp. 495-500). Institute of Industrial and Systems Engineers (IISE).

Boxall, J. B., Saul, A. J., and Skipworth, P. J. (2004). "Modeling for hydraulic capacity." *J. AWWA*, 96(4), 161-169. <https://doi.org/10.1002/j.1551-8833.2004.tb10607.x>

Braun, M., Piller, O., Deuerlein, J., Mortazavi, I., & Iollo, A. 2020. "Uncertainty quantification of water age in water supply systems by use of spectral propagation." *Journal of Hydroinformatics*, 22(1), 111-120. <https://doi.org/10.2166/hydro.2019.017>.

Caleyo, F., Velázquez, J. C., Valor, A., & Hallen, J. M. (2009). Probability distribution of pitting corrosion depth and rate in underground pipelines: A Monte Carlo study. *Corrosion Science*, 51(9), 1925-1934. <https://doi.org/10.1016/j.corsci.2009.05.019>.

Cheung, P., J. E. Van Zyl, and R. L. F. Reis. 2005. "Extension of EPANET for pressure driven demand modeling in water distribution system." In Vol. 1 of Proc., Int. Conf. Computer and Control in Water Industry, 203–208. Exeter, UK: Univ. of Exeter.

Christensen, R. T. (2009). *Age effects on iron-based pipes in water distribution systems*. Utah State University.

Christodoulou, S. E., and Fragiadakis, M. 2015. "Vulnerability assessment of water distribution networks considering performance data." *Journal of Infrastructure Systems*, 21(2), 04014040. [https://doi.org/10.1061/\(ASCE\)IS.1943-555X.0000224](https://doi.org/10.1061/(ASCE)IS.1943-555X.0000224).

Christodoulou, S., Aslani, P., & Vanrenterghem, A. (2003). A risk analysis framework for evaluating structural degradation of water mains in urban settings, using neurofuzzy systems and statistical modeling techniques. In *World Water & Environmental Resources Congress 2003* (pp. 1-9). [https://doi.org/10.1061/40685\(2003\)134](https://doi.org/10.1061/40685(2003)134).

Clark, R. M., Stafford, C. L., & Goodrich, J. A. (1982). Water distribution systems: A spatial and cost evaluation. *Journal of the Water Resources Planning and Management Division*, 108(3), 243-256. <https://doi.org/10.1061/JWRDDC.0000257>.

Colebrook, C. F. and White, C. M. (1937a). "The reduction of carrying capacity of pipes with age." *Jour. Inst. Civil Engrs.*, 7(1), 99-118.

Colebrook, C. F. and White, C. M. (1937b). "Experiments with fluid friction in roughened pipes." *Proceedings of the Royal Society*, 161(906), 367-381.

Cubrinovski, M., Bradley, B., Wotherspoon, L., Green, R., Bray, J., Wood, C., & Taylor, M. 2011. "Geotechnical aspects of the 22 February 2011 Christchurch earthquake." *Bulletin of the New Zealand Society for Earthquake Engineering*, 44(4), 205-226. <https://doi.org/10.5459/bnzsee.44.4.205-226>.

- Datta, S. K., Shah, A. H., & Wong, K. C. 1984. "Dynamic stresses and displacements in buried pipe." *Journal of engineering mechanics*, 110(10), 1451-1466. [https://doi.org/10.1061/\(ASCE\)0733-9399\(1984\)110:10\(1451\)](https://doi.org/10.1061/(ASCE)0733-9399(1984)110:10(1451)).
- Davis, P., Silva, D. D., Marlow, D., Moglia, M., Gould, S., & Burn, S. (2008). Failure prediction and optimal scheduling of replacements in asbestos cement water pipes. *Journal of Water Supply: Research and Technology—AQUA*, 57(4), 239-252. <https://doi.org/10.2166/aqua.2008.035>.
- Deb, A. K. (2002). *Prioritizing water main replacement and rehabilitation*. American Water Works Association.
- Deb, A. K., Hasit, Y. J., Grablutz, F. M., & Herz, R. K. (1998). Quantifying future rehabilitation and replacement needs of water mains. *AWWA Research Foundation*, 156.
- Didier, M., Broccardo, M., Esposito, S., & Stojadinovic, B. (2018). Seismic Resilience of a Water Distribution Network. In *Proceedings of the 16th European Conference on Earthquake Engineering (16ECEE)* (p. 11261). European Association for Earthquake Engineering. [https://doi.org/10.1061/\(ASCE\)WR.1943-5452.0000584](https://doi.org/10.1061/(ASCE)WR.1943-5452.0000584)
- Dongre, S. R., & Gupta, R. 2017. "Optimal design of water distribution network under hydraulic uncertainties." *ASCE-ASME Journal of Risk and Uncertainty in Engineering Systems, Part A: Civil Engineering*, 3(3), G4017001. <https://doi.org/10.1061/AJRUA6.0000903>.
- Eagle, J. M. (2017). PVC vs ductile iron pipe installed cost comparison calculator.
- Eidinger, J. 1998. "Water distribution system—The Loma Prieta, California, earthquake of October 17, 1989—Lifelines." USGS Professional Paper 1552-A, edited by A. J. Schiff. Washington, DC: US Government Printing Office.
- Eidinger, J. M., & Avila, E. A. (Eds.). 1999. *Guidelines for the seismic evaluation and upgrade of water transmission facilities* (Vol. 15). ASCE Publications.
- Farahmandfar, Z., Piratla, K. R., and Andrus, R. D. 2017. "Resilience evaluation of water supply networks against seismic hazards." *Journal of Pipeline Systems Engineering and Practice*, 8(1), 04016014. [https://doi.org/10.1061/\(ASCE\)PS.1949-1204.0000251](https://doi.org/10.1061/(ASCE)PS.1949-1204.0000251).
- Farshad, M. (2004). Two new criteria for the service life prediction of plastics pipes. *Polymer Testing*, 23(8), 967-972. <https://doi.org/10.1016/j.polymertesting.2004.04.010>
- Field, E. H., Seligson, H. A., Gupta, N., Gupta, V., Jordan, T. H., and Campbell, K. W. (2005). "Loss estimates for a Puente Hills blind-thrust earthquake in Los

- Angeles, California." *Earthquake Spectra*, 21(2), 329–338.
<https://doi.org/10.1193%2F1.1898332>.
- Fragiadakis, M., and Christodoulou, S. E. 2014. "Seismic reliability assessment of urban water networks." *Earthquake Engineering and Structural Dynamics*, 43 (3), 357-374.
<https://doi.org/10.1002/eqe.2348>.
- Fragiadakis, M., Christodoulou, S. E., and Vamvatsikos, D. 2013. "Reliability assessment of urban water distribution networks under seismic loads." *Water Resources Management*, 27(10), 3739-3764. <https://doi.org/10.1007/s11269-013-0378-0>.
- Goulter, I. C., & Kazemi, A. (1988). Spatial and temporal groupings of water main pipe breakage in Winnipeg. *Canadian Journal of Civil Engineering*, 15(1), 91-97. <https://doi.org/10.1139/188-010>.
- Goulter, I., Davidson, J., & Jacobs, P. (1993). Predicting water-main breakage rates. *Journal of water resources planning and management*, 119(4), 419-436.
[https://doi.org/10.1061/\(ASCE\)0733-9496\(1993\)119:4\(419\)](https://doi.org/10.1061/(ASCE)0733-9496(1993)119:4(419))
- Gustafson, J. M., & Clancy, D. V. (1999). Modeling the occurrence of breaks in cast iron water mains using methods of survival analysis. In *Proc., AWWA Annual Conf., American Water Works Association, Denver*.
- Haddaway, A. (2015). Earthquake-resitant ductile iron pipe makes US Debut in Los Angeles. *Water World*, Retrieved from <http://www.waterworld.com/articles/print,31>.
- Haghighi, A., & Asl, A. Z. 2014. "Uncertainty analysis of water supply networks using the fuzzy set theory and NSGA-II." *Engineering Applications of Artificial Intelligence*, 32, 270-282.
<https://doi.org/10.1016/j.engappai.2014.02.010>.
- Hajibabaei, M., Yousefi, A., Hesarkazzazi, S., Minaei, A., Jenewein, O., Shahandashti, M., & Sitzenfrei, R. (2023). Resilience enhancement of water distribution networks under pipe failures: a hydraulically inspired complex network approach. *AQUA—Water Infrastructure, Ecosystems and Society*, jws2023180.
- Hajibabaei, M., Yousefi, A., Hesarkazzazi, S., Roy, A., Hummel, M. A., Jenewein, O., ... & Sitzenfrei, R. (2022, August). Identification of critical pipes of water distribution networks using a hydraulically informed graph-based approach. In *World Environmental and Water Resources Congress 2022* (pp. 1041-1053).

- Herwig, H., Gloss, D., & Wenterodt, T. (2008). A new approach to understanding and modelling the influence of wall roughness on friction factors for pipe and channel flows. *Journal of Fluid Mechanics*, 613, 35-53. <https://doi.org/10.1017/S0022112008003534>
- Herz, R. K. (1996). Ageing processes and rehabilitation needs of drinking water distribution networks. *Aqua- Journal of Water Supply: Research and Technology*, 45(5), 221-231.
- Honegger, D. G., and R. T. Eguchi. 1992. *Determination of the relative vulnerabilities to seismic damage for San Diego County Water Authority (SDCWA) water transmission pipelines*. Washington, DC: FEMA.
- Hosseini, M., & Roudsari, M. T. (2010). A Study on the Effects of Surface Transverse Waves on Buried Steel Pipelines Considering the Nonlinear Behavior of Soil and Pipes. In *Pipelines 2010: Climbing New Peaks to Infrastructure Reliability: Renew, Rehab, and Reinvest* (pp. 1078-1087). [https://doi.org/10.1061/41138\(386\)103](https://doi.org/10.1061/41138(386)103).
- Huang, J. J., McBean, E. A., & James, W. 2008. Multi-objective optimization for monitoring sensor placement in water distribution systems. In *Water Distribution Systems Analysis Symposium 2006* (pp. 1-14). [https://doi.org/10.1061/40941\(247\)113](https://doi.org/10.1061/40941(247)113).
- Jaćimović, N., Stamenić, M., Kolendić, P., Đorđević, D., Radanov, B., & Vladić, L. (2015). A novel method for the inclusion of pipe roughness in the Hazen-Williams equation. *FME Transactions*, 43(1), 35-39.
- Jacobs, P., & Karney, B. (1994, May). GIS development with application to cast iron water main breakage rate. In *Proc., 2nd Int. Conf. on Water Pipeline Systems* (pp. 53-62). London, UK: Mech Eng. Publs..
- Jayaram, N., and J. W. Baker. 2009. “Correlation model for spatially distributed ground-motion intensities.” *Earthquake Eng. Struct. Dyn.* 38 (15): 1687–1708. <https://doi.org/10.1002/eqe.922>.
- Jeon, S. S., and O’Rourke, T. D. (2005). “Northridge earthquake effects on pipelines and residential buildings.” *Bulletin of the Seismological Society of America*, 95(1), 294–318. <https://doi.org/10.1785/0120040020>.
- Ji, J., Robert, D. J., Zhang, C., Zhang, D., & Kodikara, J. (2017). Probabilistic physical modelling of corroded cast iron pipes for lifetime prediction. *Structural Safety*, 64, 62-75. <https://doi.org/10.1016/j.strusafe.2016.09.004>.

- Kang, D., & Lansey, K. (2009). "Real-time demand estimation and confidence limit analysis for water distribution systems." *Journal of Hydraulic Engineering*, 135(10), 825-837. [https://doi.org/10.1061/\(ASCE\)HY.1943-7900.0000086](https://doi.org/10.1061/(ASCE)HY.1943-7900.0000086).
- Kapelan, Z. S., Savic, D. A., & Walters, G. A. 2005. "Multi objective design of water distribution systems under uncertainty." *Water Resources Research*, 41(11).
- Kettler, A. J., & Goulter, I. C. (1985). An analysis of pipe breakage in urban water distribution networks. *Canadian journal of civil engineering*, 12(2), 286-293. <https://doi.org/10.1139/185-030>.
- Kim, S., & Shahandashti, M. (2022). Diagnosing and quantifying post-disaster pipe material cost fluctuations. In *Pipelines 2022* (pp. 185-195).
- Kim, S., Abediniangerabi, B., & Shahandashti, M. (2020). Forecasting pipeline construction costs using time series methods. In *Pipelines 2020* (pp. 198-209). Reston, VA: American Society of Civil Engineers.
- Kim, S., Abediniangerabi, B., & Shahandashti, M. (2021a). Forecasting pipeline construction costs using recurrent neural networks. In *Pipelines 2021* (pp. 325-335).
- Kim, S., Abediniangerabi, B., & Shahandashti, M. (2021b). Pipeline construction cost forecasting using multivariate time series methods. *Journal of Pipeline Systems Engineering and Practice*, 12(3), 04021026.
- Knight, B. 2017. "Mexico City earthquake reconnaissance—Day 3." What's Happening. Accessed October 20, 2019. <http://www.wrkengrs.com/mexico-city-earthquake-reconnaissance-day-4/>.
- Lansey, K. E., El-Shorbagy, W., Ahmed, I., Araujo, J., & Haan, C. T. 2001. "Calibration assessment and data collection for water distribution networks." *Journal of Hydraulic Engineering*, 127(4), 270-279. [https://doi.org/10.1061/\(ASCE\)0733-9429\(2001\)127:4\(270\)](https://doi.org/10.1061/(ASCE)0733-9429(2001)127:4(270)).
- Lansey, K. E., Duan, N., Mays, L. W., & Tung, Y. K. 1989. "Water distribution system design under uncertainties." *Journal of Water Resources Planning and Management*, 115(5), 630-645. [https://doi.org/10.1061/\(ASCE\)0733-9496\(1989\)115:5\(630\)](https://doi.org/10.1061/(ASCE)0733-9496(1989)115:5(630)).
- Liu, A. W., Hu, Y. X., Zhao, F. X., Li, X. J., Takada, S., & Zhao, L. 2004. "An equivalent-boundary method for the shell analysis of buried pipelines under fault movement." *Acta Seismologica Sinica*, 17(1), 150-156. <https://doi.org/10.1007/s11589-004-0078-1>.

Luco, J. E., & De Barros, F. C. P. 1994. "Seismic response of a cylindrical shell embedded in a layered viscoelastic half-space. I: Formulation." *Earthquake engineering & structural dynamics*, 23(5), 553-567. <https://doi.org/10.1002/eqe.4290230507>.

Mamrelli, E. S., and Streicher, L. (1962). "Loss in capacity of water mains: California Section Committee Report." *J. AWWA*, 54(10), 1293-1312.

Markov, I., O'Rourke, T. D., and Grigoriu, M. (1994). "An evaluation of seismic serviceability of water supply networks with application to the San Francisco auxiliary water supply system."

Maruyama, Y., K. Kimishima, and F. Yamazaki. 2011. "Damage assessment of buried pipes due to the 2007 Niigata Chuetsu-Oki earthquake in Japan." *Journal of Earthquake and Tsunami* 5 (1): 57–70. <https://doi.org/10.1142/S179343111100098X>.

Mazumder, R. K., Fan, X., Salman, A. M., Li, Y., & Yu, X. (2020a). Framework for seismic damage and renewal cost analysis of buried water pipelines. *Journal of Pipeline Systems Engineering and Practice*, 11(4). [https://doi.org/10.1061/\(ASCE\)PS.1949-1204.0000487](https://doi.org/10.1061/(ASCE)PS.1949-1204.0000487).

Mazumder, R. K., Salman, A. M., Li, Y., & Yu, X. (2019). Reliability analysis of water distribution systems using physical probabilistic pipe failure method. *J. Water Resour. Plann. Manage.*, 145(2), 04018097. [https://doi.org/10.1061/\(ASCE\)WR.1943-5452.0001034](https://doi.org/10.1061/(ASCE)WR.1943-5452.0001034).

Mazumder, R. K., Salman, A. M., Li, Y., & Yu, X. (2020b). Seismic functionality and resilience analysis of water distribution systems. *J. Pipeline Syst. Eng. Pract.*, 11(1), 04019045. [https://doi.org/10.1061/\(ASCE\)PS.1949-1204.0000418](https://doi.org/10.1061/(ASCE)PS.1949-1204.0000418).

McMullen, L. D. (1982, May). Advanced concepts in soil evaluation for exterior pipeline corrosion. In *Proceeding of the AWWA Annual Conference*.

Melissianos, V. E., Korakitis, G. P., Gantes, C. J., & Bouckovalas, G. D. 2016. "Numerical evaluation of the effectiveness of flexible joints in buried pipelines subjected to strike-slip fault rupture." *Soil Dynamics and Earthquake Engineering*, 90, 395-410. <https://doi.org/10.1016/j.soildyn.2016.09.012>.

Newmark, N. M., & Rosenblueth, E. 1971. "Fundamentals of Earthquake Engineering. Prentice-Hall, Inc." *Englewood Cliffs, New Jersey*.

O'Rourke, T. D. 1996. "Lessons learned for lifeline engineering from major urban earthquakes." In Proc., 11th World Conf. of Earthquake Engineering. Tokyo: International Association for Earthquake Engineering.

O'Rourke, T. D., S. S. Jeon, S. Toprak, M. Cubrinovski, M. Hughes, S. Van Ballegooy, and D. Bouziou. 2014. "Earthquake response of underground pipeline networks in Christchurch, NZ." *Earthquake Spectra* 30 (1): 183–204. <https://doi.org/10.1193/030413EQS062M>.

Ormsbee, L., & Walski, T. (2016). Darcy-Weisbach versus Hazen-Williams: no calm in west palm. In *World Environmental and Water Resources Congress 2016* (pp. 455-464). <https://doi.org/10.1061/9780784479865.048>.

Pandey, P., Dongre, S., & Gupta, R. 2020. "Probabilistic and fuzzy approaches for uncertainty consideration in water distribution networks—a review." *Water Supply*, 20(1), 13-27. <https://doi.org/10.2166/ws.2019.141>.

Pineda-Porras, O., and Najafi, M. 2010. "Seismic Damage Estimation for Buried Pipelines: Challenges after Three Decades of Progress." *Journal of Pipeline Systems Engineering and Practice*, 1(1), 19–24. [https://doi.org/10.1061/\(ASCE\)PS.1949-1204.0000042](https://doi.org/10.1061/(ASCE)PS.1949-1204.0000042).

Piratla, K. R., Yerri, S. R., Yazdekhasti, S., Cho, J., Koo, D., & Matthews, J.C. 2015. "Empirical analysis of water-main failure consequences." *Procedia Engineering*, 118, 727– 734. <https://doi.org/10.1016/j.proeng.2015.08.507>.

Pouri, Z., & Heidarimozaffar, M. (2022). Spatial analysis and failure management in water distribution networks using fuzzy inference system. *Water Resources Management*, 36(6), 1783-1797.

Pudasaini, B., & Shahandashti, M. 2020a. "Topological surrogates for computationally efficient seismic robustness optimization of water pipe networks." *Computer-Aided Civil and Infrastructure Engineering*, 35(10), 1101-1114. <https://doi.org/10.1111/mice.12566>.

Pudasaini, B., & Shahandashti, S. M. 2018. "Identification of critical pipes for proactive resource-constrained seismic rehabilitation of water pipe networks." *Journal of Infrastructure Systems*, 24(4), 04018024. [https://doi.org/10.1061/\(ASCE\)IS.1943-555X.0000439](https://doi.org/10.1061/(ASCE)IS.1943-555X.0000439).

Pudasaini, B., & Shahandashti, S. M. 2020b. Seismic Resilience Enhancement of Water Pipe Networks Using Hybrid Metaheuristic Optimization." In *Pipelines 2020* (pp. 428-436). Reston, VA: American Society of Civil Engineers. <https://doi.org/10.1061/9780784483190.047>.

Pudasaini, B., and Shahandashti, M. (2021), Seismic Rehabilitation Optimization of Water Pipe Networks Considering Spatial Variabilities of Demand Criticalities and Seismic Ground Motion Intensities, *Journal of Infrastructure Systems*, ASCE, 27(4), 04021028. [https://doi.org/10.1061/\(ASCE\)IS.1943-555X.0000638](https://doi.org/10.1061/(ASCE)IS.1943-555X.0000638).

- Pudasaini, B., Shahandashti, S. M., & Razavi, M. 2017. "Identifying critical links in water supply systems subject to various earthquakes to support inspection and renewal decision making." *Computing in Civil Engineering*, 2017, 231–238. <https://doi.org/10.1061/9780784480847.029>.
- Punurai, W., & Davis, P. (2017). Prediction of asbestos cement water pipe aging and pipe prioritization using Monte Carlo simulation. *Engineering Journal*, 21(2), 1-13. <https://doi.org/10.4186/ej.2017.21.2.1>.
- Rajeev, P., Kodikara, J., Robert, D., Zeman, P., & Rajani, B. (2014). Factors contributing to large diameter water pipe failure. *Water asset management international*, 10(3), 9-14.
- Robert, D. J., Rajeev, P., Kodikara, J., & Rajani, B. (2016). Equation to predict maximum pipe stress incorporating internal and external loadings on buried pipes. *Canadian Geotechnical Journal*, 53(8), 1315-1331. <https://doi.org/10.1139/cgj-2015-0500>.
- Roy, A., Pudasaini, B., & Shahandashti, M. (2021). Seismic Vulnerability Assessment of Water Pipe Networks under Network Uncertainties. In *Pipelines 2021* (pp. 171-179).
- Roy, A., Rosenberger, J. M., & Shahandashti, M. Impact of Water Network Uncertainties on Seismic Rehabilitation Decision-Making for Water Pipelines. In *Pipelines 2023* (pp. 364-372). <https://doi.org/10.1061/9780784485019.039>.
- Roy, A., Shahandashti, M., & Rosenberger, J. M. (2022). Effects of Network Uncertainty on Seismic Vulnerability Assessment of Water Pipe Networks. *Journal of Pipeline Systems Engineering and Practice*, 13(3), 04022016. [https://doi.org/10.1061/\(ASCE\)PS.1949-1204.0000652](https://doi.org/10.1061/(ASCE)PS.1949-1204.0000652).
- RSMeans. (2018). 2018 Heavy Construction Costs Book. RSMeans Co, Rockland, MA.
- Saberi, M., Halabian, A. M., & Vafaian, M. 2011. "Numerical analysis of buried steel pipelines under earthquake excitations." In *Pan-Am CGS Geotechnical Conference*.
- Sabzkouhi, A. M., & Haghghi, A. 2016. "Uncertainty analysis of pipe-network hydraulics using a many-objective particle swarm optimization". *Journal of Hydraulic Engineering*, 142(9), 04016030. [https://doi.org/10.1061/\(ASCE\)HY.1943-7900.0001148](https://doi.org/10.1061/(ASCE)HY.1943-7900.0001148).
- Sadiq, R., Rajani, B., & Kleiner, Y. (2004). Probabilistic risk analysis of corrosion associated failures in cast iron water mains. *Reliability Engineering & System Safety*, 86(1), 1-10. <https://doi.org/10.1016/j.res.2003.12.007>.

- Scawthorn, C., Eidinger, J. M., & Schiff, A. (Eds.). 2005. *Fire following earthquake* (Vol. 26). ASCE Publications.
- Seica, M. V., & Packer, J. A. (2004). Finite element evaluation of the remaining mechanical strength of deteriorated cast iron pipes. *J. Eng. Mater. Technol.*, 126(1), 95-102. <https://doi.org/10.1115/1.1631027>.
- Seica, M. V., & Packer, J. A. (2006). Simplified numerical method to evaluate the mechanical strength of cast iron water pipes. *Journal of infrastructure systems*, 12(1), 60-67. [https://doi.org/10.1061/\(ASCE\)1076-0342\(2006\)12:1\(60\)](https://doi.org/10.1061/(ASCE)1076-0342(2006)12:1(60)).
- Seifollahi-Aghmiuni, S., Haddad, O. B., Omid, M. H., & Mariño, M. A. 2013. “Effects of pipe roughness uncertainty on water distribution network performance during its operational period.” *Water resources management*, 27(5), 1581-1599. <https://doi.org/10.1007/s11269-013-0259-6>.
- Seifollahi-Aghmiuni, S., Haddad, O. B., Omid, M. H., & Mariño, M. A. 2011. “Long-term efficiency of water networks with demand uncertainty.” In *Proceedings of the Institution of Civil Engineers-Water Management* (Vol. 164, No. 3, pp. 147-159). Thomas Telford Ltd. <https://doi.org/10.1680/wama.1000039>.
- Shaban, I. A., Eltoukhy, A. E., & Zayed, T. (2023). Systematic and scientometric analyses of predictors for modelling water pipes deterioration. *Automation in Construction*, 149, 104710. <https://doi.org/10.1016/j.autcon.2022.104710>.
- Shahandashti, M., Abediniangerabi, B., Zahed, E., & Kim, S. (2023). Investment Valuation of Construction Projects Under Uncertainty. In *Construction Analytics: Forecasting and Investment Valuation* (pp. 95-124). Cham: Springer Nature Switzerland.
- Shahandashti, M., Abediniangerabi, B., Zahed, E., & Kim, S. (2023). *Construction Analytics: Forecasting and Investment Valuation*. Springer.
- Shahandashti, S. M., & Pudasaini, B. 2019. “Proactive seismic rehabilitation decision-making for water pipe networks using simulated annealing.” *Natural Hazards Review*, 20(2), 04019003. [https://doi.org/10.1061/\(ASCE\)NH.1527-6996.0000328](https://doi.org/10.1061/(ASCE)NH.1527-6996.0000328).
- Shamir, U., & Howard, C. D. (1979). An analytic approach to scheduling pipe replacement. *Journal-American Water Works Association*, 71(5), 248-258. <https://doi.org/10.1002/j.1551-8833.1979.tb04345.x>.

- Sharp, W. W., and Walski, T. M. (1988). "Predicting internal roughness in water mains." *J. AWWA*, 80(11), 34-40. <https://doi.org/10.1002/j.1551-8833.1988.tb03132.x>.
- Sharveen, S., Roy, A., & Shahandashti, M. (2022). Risk-Averse Proactive Seismic Rehabilitation Decision-Making for Water Distribution Systems. In *Pipelines 2022* (pp. 81-90).
- Shi, P. (2006). "Seismic response modeling of water supply systems." Cornell University
- Shibu, A., & Reddy, M. J. 2011. "Uncertainty analysis of water distribution networks by fuzzy-cross entropy approach." *World Academy of Science, Engineering and Technology*, 59, 494-502.
- Shin, H., Joo, C., & Koo, J. (2016). Optimal rehabilitation model for water pipeline systems with genetic algorithm. *Procedia Engineering*, 154, 384-390. <https://doi.org/10.1016/j.proeng.2016.07.497>.
- Singhal, A. C., & Zuroff, M. S. 1990. "Analysis of underground and underwater space frames with slip joints." *Computers & structures*, 35(3), 227-237. [https://doi.org/10.1016/0045-7949\(90\)90342-Y](https://doi.org/10.1016/0045-7949(90)90342-Y).
- Sivakumar, P., Prasad, R. K., & Chandramouli, S. 2016. "Uncertainty analysis of looped water distribution networks using linked EPANET-GA method." *Water resources management*, 30(1), 331-358.
- Song, Z., Liu, W., & Shu, S. (2022). Resilience-based post-earthquake recovery optimization of water distribution networks. *International Journal of Disaster Risk Reduction*, 74, 102934. <https://doi.org/10.1016/j.ijdrr.2022.102934>
- St. Clair, A. M., & Sinha, S. (2012). State-of-the-technology review on water pipe condition, deterioration and failure rate prediction models!. *Urban Water Journal*, 9(2), 85-112. <https://doi.org/10.1080/1573062X.2011.644566>.
- Tavakoli, R., Sharifara, A., & Najafi, M. (2020, May). Artificial neural networks and adaptive neuro-fuzzy models to predict remaining useful life of water pipelines. In *World environmental and water resources congress 2020: Water, wastewater, and stormwater and water desalination and reuse* (pp. 191-204). Reston, VA: American Society of Civil Engineers.
- Thapa, B. R., H. Ishidaira, V. P. Pandey, and N. M. Shakya. 2016. "Impact assessment of Gorkha earthquake 2015 on potable water supply in Kathmandu valley: Preliminary analysis." *J. Jpn. Soc. Civ. Eng., Ser. B1 (Hydraul. Eng.)* 72 (4): I_61-I_66. https://doi.org/10.2208/jscejhe.72.I_61.

- Trautman, C. H., M. M. Khater, T. D. O'Rourke, and M. D. Grigoriu. 2013. "Modeling water supply systems for earthquake response analysis." In *Structures and stochastic methods*, 215. New York: Elsevier.
- United States Geological Survey (USGS). (2018a). "Unified Hazard Tool." Earthquake Hazards Program. <https://earthquake.usgs.gov/hazards/interactive/>.
- United States Geological Survey (USGS). (2018b). "U.S. Quaternary Faults and Folds Database." USGS. 2018a. "U.S. quaternary faults and folds database." Accessed May 10, 2020. <https://usgs.maps.arcgis.com/apps/webappviewer/index.html?id=5a6038b3a1684561a9b0aadf88412fcf>.
- Vazouras, P., Karamanos, S. A., & Dakoulas, P. 2010. "Finite element analysis of buried steel pipelines under strike-slip fault displacements." *Soil Dynamics and Earthquake Engineering*, 30(11), 1361-1376. <https://doi.org/10.1016/j.soildyn.2010.06.011>.
- Walski, T. M., & Pelliccia, A. (1982). Economic analysis of water main breaks. *Journal-American Water Works Association*, 74(3), 140-147. <https://doi.org/10.1002/j.1551-8833.1982.tb04874.x>.
- Wang, L. R. L. (1990). *A new look into the performance of water pipeline systems from 1987 Whittier Narrows, California earthquake*. Department of Civil Engineering, Old Dominion University.
- Wang, L. R., Pikul, R. R., & O'Rourke, M. J. 1982. "Imposed ground strain and buried pipelines." *Journal of the Technical Councils of ASCE*, 108(2), 259-263. <https://doi.org/10.1061/JTCAD9.0000121>.
- Wang, M., and T. Takada. 2005. "Macrosatial correlation model of seismic ground motions." *Earthquake Spectra* 21 (4): 1137–1156. <https://doi.org/10.1193%2F1.2083887>.
- Wang, W., Shi, W., & Li, C. Q. (2019). Time dependent reliability analysis for cast iron pipes subjected to pitting corrosion. *International Journal of Pressure Vessels and Piping*, 175, 103935. <https://doi.org/10.1016/j.ijpvp.2019.103935>.
- Wang, Y., Au, S.-K., and Fu, Q. (2010). "Seismic risk assessment and mitigation of water supply systems." *Earthquake Spectra*, Earthquake Engineering Research Institute, 26(1), 257–274. <https://doi.org/10.1193/1.3276900>.
- Water Distribution System Operations. 2013. "Database." Accessed September 1, 2019. <http://www.uky.edu/WDST/database.html>.

- Watson, T. G., Christian, C. D., Mason, A. J., Smith, M. H., & Meyer, R. (2004). Bayesian-based pipe failure model. *Journal of Hydroinformatics*, 6(4), 259-264. <https://doi.org/10.2166/hydro.2004.0019>.
- Weatherill, G., V. Silva, H. Crowley, and P. Bazzurro. 2013. "Exploring strategies for portfolio analysis in probabilistic seismic loss estimation." In Proc., Vienna Congress on Recent Advances in Earthquake Engineering and Structural Dynamics, 28–30. Vienna, Austria: Vienna Univ. of Technology.
- Williams, G. S., and Hazen, A. (1960). Hydraulic tables, Wiley, New York.
- Xu, C., & Goulter, I. C. 1998. "Probabilistic model for water distribution reliability." *Journal of Water Resources Planning and Management*, 124(4), 218-228. [https://doi.org/10.1061/\(ASCE\)0733-9496\(1998\)124:4\(218\)](https://doi.org/10.1061/(ASCE)0733-9496(1998)124:4(218)).
- Yerri, S. R., Piratla, K. R., Matthews, J. C., Yazdekhasti, S., Cho, J., & Koo, D. 2017. Empirical analysis of large diameter water main break consequences. *Resources, Conservation and Recycling*, 123, 242-248. <https://doi.org/10.1016/j.resconrec.2016.03.015>.
- Yoo, D. G., Jung, D., Kang, D., Kim, J. H., & Lansey, K. 2016. "Seismic hazard assessment model for urban water supply networks." *Journal of Water Resources Planning and Management*, 142(2), 04015055. [https://doi.org/10.1061/\(ASCE\)WR.1943-5452.0000584](https://doi.org/10.1061/(ASCE)WR.1943-5452.0000584).
- Zahed, S. E., Shahandashti, S. M., & Diltz, J. D. (2020). Investment valuation of underground freight transportation systems under uncertainty. *Journal of Infrastructure Systems*, 26(3), 04020029.
- Zanini, M. A., Faleschini, F., & Pellegrino, C. 2017. Probabilistic seismic risk forecasting of aging bridge networks. *Engineering Structures*, 136, 219-232. <https://doi.org/10.1016/j.engstruct.2017.01.029>.
- Zanini, M. A., Vianello, C., Faleschini, F., Hofer, L., & Maschio, G. 2016. "A framework for probabilistic seismic risk assessment of NG distribution networks." *Chemical Engineering Transactions*, 53, 163-168.